Phytotoxicity and Innate Immune Responses Induced by Nep1-Like Proteins [W]

Dinah Qutob,[a,1] Birgit Kemmerling,[b,1] Frédéric Brunner,[b,1] Isabell Küfner,[b] Stefan Engelhardt,[b] Andrea A. Gust,[b] Borries Luberacki,[b] Hanns Ulrich Seitz,[b] Dietmar Stahl,[c] Thomas Rauhut,[d] Erich Glawischnig,[d] Gabriele Schween,[e] Benoit Lacombe,[f] Naohide Watanabe,[g] Eric Lam,[g] Rita Schlichting,[h] Dierk Scheel,[h] Katja Nau,[i] Gabriele Dodt,[i] David Hubert,[j] Mark Gijzen,[a] and Thorsten Nürnberger[b,2]

[a] Agriculture and Agri-Food Canada, London ON N5V 4T3, Canada
[b] Center for Plant Molecular Biology–Plant Biochemistry, University of Tübingen, D-72076 Tübingen, Germany
[c] PLANTA Angewandte Pflanzengenetik und Biotechnologie, D-37555 Einbeck, Germany
[d] Department of Genetics, Technical University Munich, D-85350 Freising, Germany
[e] Department of Plant Biotechnology, University of Freiburg, D-79104 Freiburg, Germany
[f] Unité Mixte de Recherches Biochimie et Physiologie Moleculaire des Plantes, AgroM, Centre National de la Recherche Scientifique, Institut National de la Recherche Agronomique, Université Montpellier II, F-34060 Montpellier, France
[g] Biotechnology Center for Agriculture and the Environment, Rutgers, The State University of New Jersey, New Brunswick, New Jersey 08901-8520
[h] Department of Stress and Developmental Biology, Leibniz-Institute of Plant Biochemistry, D-06120 Halle/Saale, Germany
[i] Department of Cellular Biochemistry, Interfaculty Institute of Biochemistry, University of Tübingen, D-72076 Tübingen, Germany
[j] Department of Biology, University of North Carolina, Chapel Hill, North Carolina 27599

We show that oomycete-derived Nep1 (for necrosis and ethylene-inducing peptide1)–like proteins (NLPs) trigger a comprehensive immune response in *Arabidopsis thaliana*, comprising posttranslational activation of mitogen-activated protein kinase activity, deposition of callose, production of nitric oxide, reactive oxygen intermediates, ethylene, and the phytoalexin camalexin, as well as cell death. Transcript profiling experiments revealed that NLPs trigger extensive reprogramming of the *Arabidopsis* transcriptome closely resembling that evoked by bacteria-derived flagellin. NLP-induced cell death is an active, light-dependent process requiring HSP90 but not caspase activity, salicylic acid, jasmonic acid, ethylene, or functional SGT1a/SGT1b. Studies on animal, yeast, moss, and plant cells revealed that sensitivity to NLPs is not a general characteristic of phospholipid bilayer systems but appears to be restricted to dicot plants. NLP-induced cell death does not require an intact plant cell wall, and ectopic expression of NLP in dicot plants resulted in cell death only when the protein was delivered to the apoplast. Our findings strongly suggest that NLP-induced necrosis requires interaction with a target site that is unique to the extracytoplasmic side of dicot plant plasma membranes. We propose that NLPs play dual roles in plant pathogen interactions as toxin-like virulence factors and as triggers of plant innate immune responses.

INTRODUCTION

Both plants and animals possess innate defense mechanisms to resist microbial infection (Akira et al., 2006; Chisholm et al., 2006). Although innate immune systems from both lineages share conceptual and mechanistic features, they are likely the result of convergent evolution (Ausubel, 2005). Efficient plant disease resistance is based on two evolutionarily linked forms of innate immunity. The primary plant immune response is referred to as PAMP-triggered immunity (PTI) and has evolved to recognize invariant structures of microbial surfaces, termed pathogen-

or microbe-associated molecular patterns (PAMPs/MAMPs) (Nürnberger et al., 2004; Ausubel, 2005; Zipfel and Felix, 2005; Chisholm et al., 2006). Subversion of PTI by microbial effectors is believed to be one of the key strategies of successful pathogens to grow and multiply on host plants (Alfano and Collmer, 2004). In the coevolution of host–microbe interactions, individual plant cultivars have acquired resistance (R) proteins that guard microbial effector-mediated perturbations of host cell functions and thereby trigger plant immune responses. This type of plant defense is referred to as effector-triggered immunity (ETI) and is synonymous to pathogen race/host plant cultivar-specific plant disease resistance (Ausubel, 2005; Chisholm et al., 2006).

Activation of either type of plant immunity requires sensitive host perception systems that recognize microbe-derived determinants of nonself (Chisholm et al., 2006). PTI is initiated upon recognition of conserved microbial structures (PAMPs) by plant surface receptors (Zipfel and Felix, 2005). Importantly, PAMP-induced immune responses have recently been demonstrated to contribute to basal resistance of host plants against virulent

pathogens and have been shown to be crucial for the stability of nonhost resistance (Zipfel et al., 2004, 2006; Kim et al., 2005; He et al., 2006). Activation of plant cultivar-specific disease resistance is mediated by direct or indirect recognition of microbial effectors through R proteins. Microbial effectors that are supposed to serve as virulence factors in the absence of their cognate plant R protein are thus turned into avirulence (AVR) factors (Alfano and Collmer, 2004). This type of effector recognition has been genetically characterized as gene-for-gene resistance (Chisholm et al., 2006).

In addition to PAMP or AVR effector-mediated nonself recognition, breakdown products of the plant cell wall are known to serve as endogenous danger signals that monitor distress of host structures and elicit plant immune responses (Vorwerk et al., 2004). Such plant-derived elicitors that are probably released by glucohydrolytic activities from attacking microbes may conceptually be compared with animal stress proteins that are produced upon microbial infection and function as danger signals, alerting the immune system by induction of innate immune responses (Gallucci and Matzinger, 2001).

Microbial toxin-induced plant innate immunity constitutes a seemingly paradoxical phenomenon that is not well understood. Phytopathogenic microorganisms produce a wide range of cytolytic compounds that function as key virulence determinants (van't Slot and Knogge, 2002; Glazebrook, 2005). In particular, phytopathogenic necrotrophic fungi synthesize numerous host selective and host nonselective toxins that facilitate killing of host plant tissue (van't Slot and Knogge, 2002; Wolpert et al., 2002; Gijzen and Nürnberger, 2006). An intriguing characteristic of many of these toxins is that they trigger individual facets of the plant defensive arsenal. For example, certain *Fusarium* spp produce the sphinganine toxin fumonisin B1 (FB1) that elicits cytolysis of plant and animal cells most probably through competitive inhibition of ceramide synthase, a key enzyme in sphingolipid biosynthesis (Wang et al., 1996; Tolleson et al., 1999). In addition to cell death, FB1 triggers accumulation of reactive oxygen species (ROS), deposition of callose, defense-related gene expression, and production of the phytoalexin camalexin in *Arabidopsis thaliana* (Asai et al., 2000; Stone et al., 2000). Likewise, the cell death–inducing toxins fusicoccin from *Fusicoccum amygdali* or AAL toxin from *Alternaria alternata* trigger expression of pathogenesis-related (PR) genes in tomato (*Solanum lycopersicum*) or *Arabidopsis*, respectively (Schaller and Oecking, 1999; Gechev et al., 2004). Moreover, the host selective cell death–inducing toxin victorin from *Cochliobolus victoriae* was shown to elicit the production of avenanthramide phytoalexins in oat (*Avena sativa*) (Tada et al., 2005). In all cases, it remains unclear whether plant immune responses constitute an unavoidable consequence of toxin action or, alternatively, if activation of plant defense is essential for the virulence function of fungal toxins. In summary, cytolytic toxins appear to play dual roles in plant–pathogen interactions as virulence determinants and, like PAMPs or AVR effectors, act as nonself recognition determinants for the activation of plant innate immune responses (Gijzen and Nürnberger, 2006). Such an activity spectrum is not unique to plants as various bacteria-derived cytolytic toxins were shown to trigger both innate immune responses and cell death in mammalian cells (Huffman et al., 2004; Srivastava et al., 2005).

Programmed cell death (PCD) is a common consequence in both compatible and incompatible plant–pathogen interactions (Greenberg and Yao, 2004; Glazebrook, 2005). The hypersensitive response (HR) is a type of PCD that is frequently observed in ETI. PAMPs may also cause PCD by direct or indirect interactions with pattern recognition receptors. For example, an ethylene-inducing xylanase from *Trichoderma viride* causes PCD in tomato cells, apparently by binding to a cell surface receptor (Ron and Avni, 2004). Less is known about the host cell death that occurs in susceptible plants, but increasing evidence suggests that resistance and susceptibility-associated PCD share regulatory and mechanistic features (Greenberg and Yao, 2004). The timely induction of PCD may present a formidable barrier to pathogen establishment, especially to biotrophic organisms that rely on living host cells for nutrients. Defense strategies that culminate in PCD may nonetheless become a dangerous liability to the host when it is engaged with necrotrophic pathogens (Greenberg and Yao, 2004). Inappropriate PCD can accelerate disease and foster the growth of necrotrophic pathogens that live off of dead or dying cells (Gijzen and Nürnberger, 2006).

Fusarium oxysporum f. sp *erythroxyli*–derived Nep1 constitutes the founding member of a family of microbial proteins that are secreted by plant pathogenic oomycetes, fungi, and bacteria (Pemberton and Salmond, 2004; Gijzen and Nürnberger, 2006; Kamoun, 2006). Nep1-like proteins (NLPs) trigger plant defense responses and, subsequently, cell death. NLPs are relatively small proteins of ∼24 kD that exhibit a high degree of sequence conservation, including a pair of Cys residues that are predicted to form a disulfide bridge. Moreover, their necrosis and defense-inducing activity is heat-labile, suggesting that an intact three-dimensional structure and enzymatic activity are important for NLP activity. Among angiosperms, dicotyledonous plants are considered susceptible to the effects of NLPs, whereas monocots are insensitive (Bailey, 1995; Veit et al., 2001; Fellbrich et al., 2002; Keates et al., 2003; Mattinen et al., 2004; Pemberton et al., 2005). Studies in various dicot plants have shown that NLPs can activate defense-associated responses, such as the synthesis of phytoalexins and ethylene, the accumulation of defense-related transcripts, and cell death (Veit et al., 2001; Fellbrich et al., 2002; Keates et al., 2003; Mattinen et al., 2004; Pemberton et al., 2005; Bae et al., 2006). Despite the fact that NLPs rapidly activate plant defense responses, these proteins have been shown to contribute to the virulence of necrotrophic fungal and bacterial pathogens. Several arguments support the view that NLP action on plants may resemble that of host nonselective toxins. (1) NLPs exert cytolytic activity that causes cell maceration and death in dicotyledonous plants in a manner that is similar to disease symptom development during natural infections of host plants (Pemberton and Salmond, 2004; Gijzen and Nürnberger, 2006; Kamoun, 2006). (2) Loss or gain of NLP expression affects virulence and disease symptom development in dicotyledonous plants, suggesting that NLPs act as positive virulence factors during infection of plants (Amsellem et al., 2002; Mattinen et al., 2004; Pemberton et al., 2005). For example, inactivation of the NLP-encoding genes (NLP$_{Ec}$) in different *Erwinia carotovora* strains resulted in significantly reduced levels of soft rot disease on potato (*Solanum tuberosum*), indicating that NLP$_{Ec}$ contributes to bacterial fitness and disease symptom development

(Mattinen et al., 2004; Pemberton et al., 2005). Likewise, over-expression of Nep1 in the hypovirulent fungus *Colletotrichum coccodes* dramatically increased its aggressiveness toward the host plant *Abutilon theophrasti* and even enlarged the host range of this pathogen (Amsellem et al., 2002). (3) Finally, increased transcript accumulation of a *Phytophthora sojae* NLP (NLP$_{Ps}$) coincided closely with the transition from biotrophy to necrotrophy during infection of soybean (*Glycine max*) (Qutob et al., 2002), also suggesting that NLP$_{Ps}$ may act as a virulence factor by facilitating host cell death.

Here, we show that NLPs exhibit a wide taxonomic distribution pattern that is unusual for microbial virulence factors. This, together with the wealth of NLP-sensitive plants, makes these proteins well suited to serve as nonself recognition determinants in plant–pathogen interactions. We present a comprehensive analysis of innate defense reactions that are mounted in intact *Arabidopsis* plants in response to various oomycete-derived NLPs. Our analyses suggest that NLPs trigger a spectrum of plant immune responses that largely resembles that of regular PAMPs, such as bacterial flagellin. In addition to alerting the plant immune system, NLPs function as toxins by causing host cell death in dicotyledonous plants. NLP-mediated necrosis is an active process with features that are both shared and distinct from PCD mediated by other known triggers of plant cell death. Moreover, NLP-induced cell death is light dependent and requires membrane side-specific interaction with a dicot plant–specific target site.

RESULTS

Taxonomic Diversity of the NLP Protein Family

The NPP1 domain has been recognized by the Conserved Domain Database in GenBank, by Pfam (PF05630), and by InterPro (IPR008701) as an identifiable protein motif. NPP1 refers to the original name of the *Phytophthora parasitica*–derived NLP$_{Pp}$ (Fellbrich et al., 2002). Databases of known and predicted protein sequences in GenBank were searched using the Conserved Domain Database to find sequences containing an NPP1 domain or a fragment thereof. A total of 62 protein sequences encoding NLPs could be retrieved that upon correction for redundant sequences represent 44 different NLPs from 22 species (Figure 1). Thus, such proteins appear to be common molecular patterns that are associated with both prokaryotic and eukaryotic microorganisms but cannot be found in the genomes of any higher organisms, including plants (see Supplemental Figures 1 and 2 online). NLP sequences are present in gram-negative and gram-positive bacteria as well as among fungi and stramenopiles but are predominantly present in organisms that at least partially rely on heterotrophic (either hemibiotrophic, necrotrophic, or saprophytic) growth. Consequently, many plant pathogens that favor such an infection strategy were shown to harbor NLP sequences. In contrast with certain saprophytic and plant pathogenic bacterial species that possess a single NLP-encoding gene, phytopathogenic fungi or oomycetes (belonging to the eukaryotic stramenopile lineage) were shown to harbor NLP-encoding gene families (see Supplemental Figure 2 online). A total of 10 NLP-encoding sequences were reported from four plant pathogenic

fungal species, while 16 sequence entries were found for four species of the oomycete genus *Phytophthora*, all of which are destructive plant pathogens. This apparent gene diversification suggests that NLPs are important to the hemibiotrophic or necrotrophic lifestyle of fungi and oomycetes in general and of *Phytophthora* species in particular.

NLPs Trigger a Comprehensive Immune Response in *Arabidopsis*

NLPs of bacterial, fungal, and oomycete origin trigger cell death and other defense-associated responses in numerous dicotyledonous plant species (Pemberton and Salmond, 2004; Gijzen and Nürnberger, 2006). Because of the wide distribution of NLP sequences among microbial taxa and the broad sensitivity spectrum of potential hosts, NLPs are predestined to act as nonself recognition determinants during the activation of innate immune responses in plants. Because a detailed study of the complexity of NLP-induced immunity in one particular plant species is missing, we conducted a comprehensive characterization of local defense-associated responses in the dicot model plant *Arabidopsis.* Previously, the NLP-mediated production of ROS and ethylene and the accumulation of transcripts encoding pathogenesis-related proteins, necrotic lesion formation, and callose apposition at the interface between necrotic and healthy plant tissues have been documented (Veit et al., 2001; Fellbrich et al., 2002; Keates et al., 2003). Here, we focus on the characterization of additional early plant responses that in part constitute elements of NLP-induced signal transduction cascades as well as on NLP$_{Pp}$-induced alterations in the *Arabidopsis* transcriptome.

Posttranslational activation of mitogen-activated protein kinase (MAPK) activity is commonly associated with plant immunity (Pedley and Martin, 2005). Infiltration of recombinant NLP from *P. parasitica* (NLP$_{Pp}$) into *Arabidopsis* leaves and subsequent immunodetection of MAPK activity using an antibody specific for the enzymatically active form of MAPK was performed. As shown in Figure 2A, NLP$_{Pp}$ treatment resulted in rapid but transient phosphorylation of two MAPK species of 44 and 46 kD, respectively. This pattern closely resembles that obtained upon stimulation of an *Arabidopsis* cell culture with the PAMP, flg22 (Nühse et al., 2000). Production of nitric oxide (NO) is another hallmark of immune responses in both animals and plants (Zeidler et al., 2004). As shown in Figure 2B, treatment with NLP$_{Pp}$ of *Arabidopsis* resulted in a dosage-dependent increase in NO production within 30 min. Likewise, application of 1 µM flg22 triggered an NO burst similar to that produced by NLP$_{Pp}$ (data not shown). While MAPK activation and NO production are likely implicated in signal transduction processes, production of the antimicrobial phytoalexin, camalexin, is part of the executing arsenal of the plant defense system. Both NLP$_{Ps}$ and NLP from *Pythium aphanidermatum* (NLP$_{Pya}$) triggered the production of similar camalexin levels in *Arabidopsis* plants (Figure 2C). The maximum concentration produced was 93.9 µg/g dry mass in plants that were treated with NLP$_{Ps}$ for 48 h. In addition, both NLP preparations initiated camalexin production with comparable kinetics. The earliest time point when substantial amounts of the phytoalexin were found to accumulate was 8 h after infiltration.
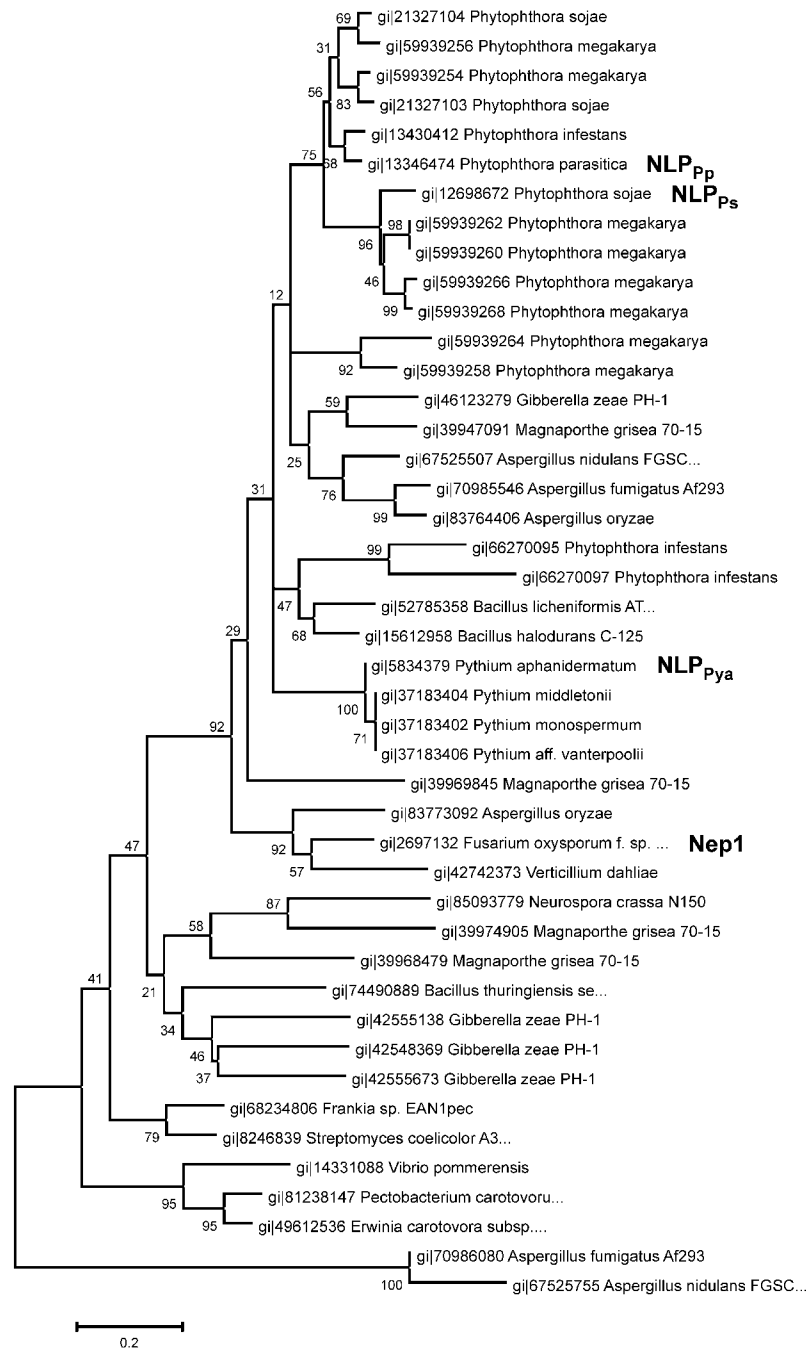
Figure 1. Phylogeny of NLPs.

The Nep1 protein sequence and 43 related sequences are shown. The scale bar represents 20% weighted sequence divergence. GenBank identifier numbers for each protein sequence are shown along with the species of origin. Sequences with special relevance to this study are additionally labeled: Nep1, necrosis and ethylene inducing peptide 1; NLP$_{Pp}$, NLP from *Phytophthora parasitica*; NLP$_{Ps}$, NLP from *Phytophthora sojae*; NLP$_{Pya}$, NLP from *Pythium aphanidermatum.*

Stimulus-induced alterations in transcriptional programs are important for the ability of living cells to respond to changes in their environment. To elucidate NLP$_{Pp}$-induced changes in the transcriptome of *Arabidopsis* plants, we obtained expression estimates from plant samples harvested 1 or 4 h after infiltration.

These time points were chosen because they precede the onset of NLP$_{Pp}$-induced cell death. Thus, gene expression due to death-related signals should be minimized under these conditions. We used Affymetrix ATH1 arrays, which contain 22,746 probe sets, corresponding to >80% of annotated genes. For
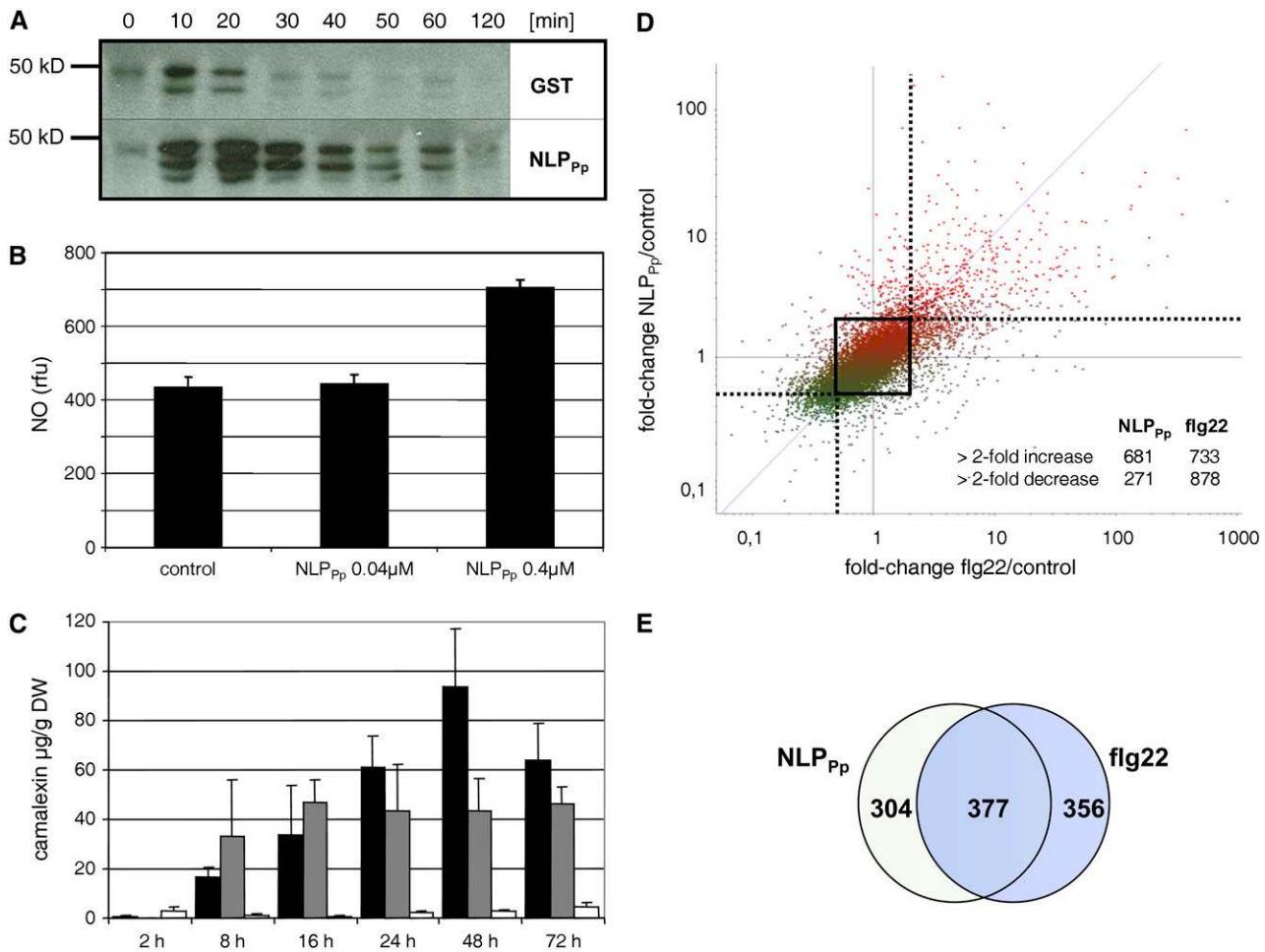
Figure 2. NLP-Induced Activation of Plant Immune Responses in *Arabidopsis*.

(A) Five-week-old *Arabidopsis* plants were infiltrated with 2 μM recombinant NLP$_{Pp}$ or glutathione *S*-transferase (GST) as control (Fellbrich et al., 2002) for the times indicated. Proteins were extracted and subjected to protein blot analysis using a 1:1000 dilution of phospho-p44/42 MAP kinase antibody as described in Methods.

(B) *Arabidopsis* cell culture aliquots (2.5 $\times$ 10^4/50 μL) were treated with the indicated recombinant NLP$_{Pp}$ concentrations or *Escherichia coli* protein extracts as control. NO production is given as relative fluorescence units (rfu).

(C) Camalexin accumulation in 5-week-old *Arabidopsis* rosette leaves after infiltration with 2 μM recombinant NLP$_{Ps}$ (black bars), 2 μM recombinant NLP$_{Pya}$ (gray bars), or protein renaturation buffer as control (white bars). Camalexin was extracted at the time points indicated and determined as described in Methods. All experiments shown in **(A)** to **(C)** were performed at least three times with identical results. Data in **(B)** and **(C)** show average values + SD.

(D) and **(E)** Transcriptome analysis in 5-week-old *Arabidopsis* plants treated with 1 μM recombinant NLP$_{Pp}$ (GST as control) or 1 μM synthetic flg22 (water as control). All experiments were performed in triplicate, and expression levels for each probe set were analyzed as described in Materials.

(D) Behavior of 12,557 genes significantly expressed at 1 or 4 h after treatments. Scatterplot analysis of fold induction of the probe sets for NLP$_{Pp}$ trials (4 h) versus fold induction for flg22 trials (4 h). For each treatment versus control condition, genes that changed were assigned based on a one-way analysis of variance (ANOVA) test combined with a Benjamini and Hochberg false discovery rate algorithm. The numbers given in the inset refer to those genes of which expression was statistically significantly altered more than twofold at least at one of the two time points tested. The rectangular box comprises those genes that are unaltered in expression upon stimulation. Probe sets in areas enclosed by dotted lines are coordinately upregulated (red dots) or downregulated (green dots).

(E) Venn diagram showing the total number of genes that are coordinately expressed by both stimuli (overlap) or of which expression is specifically upregulated by either NLP$_{Pp}$ or flg22 treatment.

comparative reasons, global expression profiles triggered by the bacterial PAMP, flg22, which activates PTI responses in *Arabidopsis* through binding to its cognate pattern recognition receptor, FLS2 (Gomez-Gomez and Boller, 2000), were obtained. The prime incentive for performing comparative microarray analyses on elicited plants was to determine whether gene sets responding to flg22 (Zipfel et al., 2004) were also responsive to NLP$_{Pp}$ treatment. Positive evidence would support the notion that toxin-like proteins, such as NLPs, and genuine PAMPs, such as flg22, trigger similar alterations in global expression profiles.

An overall analysis of NLP$_{Pp}$ and flg22-specific transcriptome profiles revealed a high degree of coexpression, strongly suggesting that both stimuli have a comparable impact on plant gene expression (Figure 2D). The number of genes of which expression was found to be induced more than twofold upon either 1 or 4 h of NLP$_{Pp}$ treatment was 681 (3% of all genes arrayed), while the corresponding number of flg22-induced genes was 733 (3.2%) (Figure 2E). Individual data sets of NLP$_{Pp}$ or flg22-induced genes are provided in Supplemental Tables 1 to 5 online. Importantly, expression of 377 out of 681 genes (55.4%) induced by NLP$_{Pp}$ treatment was similarly induced upon recognition of flg22. Again, this finding strongly supports the view that microbe-derived toxin-like molecules, such as NLP, and genuine PAMPs trigger similar alterations in the plant transcriptome. A classification of the encoded proteins according to their proposed molecular function showed that each elicitor not only activated the expression of largely overlapping gene sets but also of genes that fall into the same functional categories (data not shown). The latter finding is important because it is also based upon the analysis of the nonoverlapping gene set.

A detailed analysis of NLP$_{Pp}$-induced genes revealed two important findings. First, numerous genes encoding receptor-like protein kinases, disease resistance-like proteins, and pathogenesis/defense-related proteins were responsive to NLP$_{Pp}$ treatment (Table 1). Second, expression of the vast majority of these genes was responsive to NLP$_{Pp}$ but was also affected by flg22 treatment. For example, seven out of 16 genes encoding Leu-rich repeat receptor–like protein kinases (LRR-RLKs) were induced by either stimulus. Expression of the FLS2 gene was induced by flg22 but was not induced above threshold levels by NLP$_{Pp}$ (see Supplemental Tables 3 and 4 online). LRR-RLKs build a large monophyletic gene family in *Arabidopsis*, comprising ~235 members (Shiu et al., 2004), two of which have been implicated in noncultivar-specific plant immunity (Gomez-Gomez and Boller, 2000; Zipfel et al., 2006). Likewise, numerous LRR-containing disease resistance proteins are known to contribute to plant cultivar-specific immunity (Nürnberger et al., 2004; Zipfel and Felix, 2005). Although it is premature to assign gene functions merely on the basis of stimulus-induced alterations in the corresponding transcript profiles, it is assumed that many LRR-RLKs contribute to nonself recognition and microbial containment during attempted infection (Zipfel and Felix, 2005; Chisholm et al., 2006).

The WRKY family of transcription factors comprises a third class of signal transduction components that are associated with plant immunity. Expression of WRKY genes known to be induced during bacterial infection or flg22 treatment was also enhanced in NLP$_{Pp}$-treated plants (Table 1). Moreover, mitogen-activated

protein kinase 3 (MPK3), another component of flg22-induced signaling cascades (Asai et al., 2002), was responsive to flg22 and NLP$_{Pp}$. In addition, numerous *PR* or defense-associated genes (chitinase, peroxidase, polygalacturonase-inhibiting protein, proteinase inhibitor, and biosynthetic enzymes of the general phenylpropanoid pathway, such as Phe ammonia lyase 1 and 4-coumarate-CoA ligase 1 and 2) were induced to variable extent by either stimulus. Transcript levels of genes encoding respiratory burst oxidase isoforms D (*RbohD*) and F (*RbohF*), both of which have been implicated in ETI against *Pseudomonas syringae* pv *tomato* and *Hyaloperonospora parasitica* (Torres and Dangl, 2005), increased upon NLP$_{Pp}$ treatment, whereas expression of other *Rboh* isoform-encoding genes was not affected.

As shown in Figure 2C, infiltration of NLP$_{Ps}$ or NLP$_{Pya}$ induced camalexin production. Based on our microarray experiments, we conclude that camalexin biosynthesis is preceded by production of the corresponding biosynthetic enzymes. Transcripts encoding anthranilate synthase (*ASA1*), Trp synthase (*TSA1*), and cytochrome P450 enzymes (*PAD3/CYP71B15* and *CYP79B2*) were found to accumulate in plants infiltrated with NLP$_{Pp}$ at times before camalexin accumulation.

The plant hormones ethylene, jasmonic acid (JA), and salicylic acid (SA) have been implicated in various aspects of plant disease resistance signaling (Pieterse and Van Loon, 2004). To analyze a possible involvement of hormone signaling in NLP$_{Pp}$-induced plant responses, we investigated the expression of hormone biosynthesis enzyme-encoding genes. Genes encoding ethylene biosynthesis enzymes 1-aminocyclopropane-1-carboxylate (ACC) synthase (*ACS*) and ACC oxidase were strongly induced upon NLP$_{Pp}$ treatment. These results are in good agreement with previous studies that showed NLP$_{Pp}$-induced ethylene production (Fellbrich et al., 2002). Likewise, transcript levels of some genes encoding ethylene response proteins or ethylene-responsive element binding proteins were altered in plants treated with NLP$_{Pp}$. Strikingly, none of the genes encoding various isoforms of JA biosynthetic enzymes were altered in expression, such as phospholipase A, lipoxygenase, allene oxide synthase, allene oxide cyclase, 12-oxophytodienoate reductase, or jasmonate-*O*-methyl transferase (see Supplemental Tables 1 and 2 online). These results indicate that NLP$_{Pp}$ treatment does not rapidly activate de novo synthesis of JA biosynthetic enzymes in plants. By contrast, accumulation of transcripts encoding SA biosynthetic enzymes was observed as transcripts for isochorismate synthase 1 (*ICS1/SID2*) and Phe ammonia lyase accumulated rapidly in plants treated with NLP$_{Pp}$ (Table 1).

Among the 304 genes that were induced at early time points by NLP$_{Pp}$, but not by flg22 (Figure 2D; see Supplemental Tables 1 and 2 online), there were 20 sequences encoding PR proteins and disease resistance-like proteins with LRR, LRR-RLK, or TIR-NBS signatures. Moreover, four cytochrome P450-encoding genes and five NLP$_{Pp}$-responsive genes that encode lipases, a lipid-modifying enzyme, or a phospholipid transport protein were found.

Reduction of plant growth in the presence of flg22 constitutes a surprising yet inexplicable phenomenon that facilitated the identification and isolation of the flagellin receptor FLS2 by forward genetic screening (Gomez-Gomez and Boller, 2000; Zipfel et al., 2006). To test whether growth and development of

Table 1. NLP$_{Pp}$ or flg22-Induced Genes with Known or Putative Roles in Immunity-Related Signal Perception, Signal Transduction, Pathogen Defense Execution, and Hormone Metabolism

Arabidopsis Genome Initiative	Description	Name	NLP$_{Pp}$ 1 h	NLP$_{Pp}$ 4 h	*flg22* 1 h	*flg22* 4 h
Receptor-Like Kinases			(Fold Expression/Adjusted P Value)			
Lectin RLKs						
AT3G53810	Lectin protein kinase		–	4.3/0.019	–	–
AT3G59700	Lectin protein kinase	At LECRK	2.2/0.042	7.4/0.028	4.7/0.012	9.8/0.003
AT4G04960	Lectin protein kinase		–	3.8/0.028	–	2.6/0.010
AT4G28350	Lectin protein kinase		–	5.5/0.020	3.7/0.007	–
AT5G01550	Lectin protein kinase		–	10.7/0.020	–	–
AT5G35370	Lectin protein kinase		–	2.3/0.040	2.2/0.034	2.8/0.025
AT5G60270	Lectin protein kinase		–	2.9/0.049	3/0.007	–
S-locus RLKs						
AT1G61360	S-locus lectin protein kinase		3.1/0.025	2.1/0.020	3.3/0.019	6.9/0.010
AT1G61370	S-locus lectin protein kinase		2.2/0.007	3.9/0.013	2.9/0.004	–
AT1G61420	S-locus lectin protein kinase		–	3.3/0.025	2.4/0.010	–
AT2G19130	S-locus lectin protein kinase		5.7/0.011	–	4.2/0.007	–
AT4G21390	S-locus lectin protein kinase		3/0.017	9.4/0.019	6.5/0.007	–
AT4G27300	S-locus protein kinase		2.2/0.032	–	–	–
LRR-RLKs						
AT1G17750	LRR transmembrane protein kinase		2.8/0.030	–	–	–
AT1G29750	LRR transmembrane protein kinase	RKF1	–	2.4/0.025	–	–
AT1G35710	LRR transmembrane protein kinase		2.2/0.024	–	–	–
AT1G51820	LRR protein kinase		–	6.6/0.035	–	–
AT1G51890	LRR protein kinase		–	6.9/0.040	–	–
AT1G53430	LRR protein kinase		–	2.9/0.025	–	3.5/0.019
AT1G56120	LRR protein kinase		2.2/0.014	2.9/0.028	4/0.006	5.8/0.018
AT1G69270	LRR protein kinase	RPK1	2.7/0.012	–	–	–
AT1G74360	LRR protein kinase		2/0.047	7/0.019	3.3/0.014	6.3/0.011
AT2G02220	LRR protein kinase		–	5.4/0.029	4.9/0.009	13.6/0.012
AT2G19190	Light/senescence-responsive protein kinase	SIRK/FRK	–	7.1/0.034	–	–
AT3G13380	LRR protein kinase	BRL3	2.2/0.049	–	–	2.7/0.024
AT3G28450	LRR protein kinase		–	2/0.028	–	–
AT4G39270	LRR transmembrane protein kinase		–	4.2/0.020	–	–
AT5G01950	LRR transmembrane protein kinase		2.2/0.025	–	3.4/0.007	–
AT5G25930	LRR protein kinase		–	9/0.020	2/0.007	7/0.038
Other RLKs						
AT1G16090	Wall-associated kinase-related	WAKL7	4.4/0.010	19.5/0.019	–	–
AT1G79670	Wall-associated kinase	RFO1/WAKL	–	2.2/0.027	3.7/0.048	–
AT3G22060	Receptor protein kinase-related		2.1/0.020	4.2/0.020	4/0.015	21.4/0.008
AT4G18250	Receptor Ser/Thr kinase		–	9.9/0.050	3.3/0.040	–
Disease Resistance-Like Genes						
AT1G11310	Seven transmembrane MLO family protein 2	MLO2	3.3/0.036	–	4.8/0.026	–
AT1G61560	Seven transmembrane MLO family protein 6	MLO6	14/0.028	13.2/0.023	15.5/0.005	–
AT2G39200	Seven transmembrane MLO family protein 12	MLO12	2.3/0.024	6.6/0.025	6.5/0.007	77/0.009
AT1G22900	Disease resistance-responsive family protein		–	3.6/0.023	–	–
AT1G55210	Disease resistance response		–	4.6/0.027	–	–
AT1G57630	Disease resistance protein (TIR class)		–	6.1/0.019	2.9/0.019	9.4/0.013
AT1G63350	Disease resistance protein (CC-NBS-LRR class)		–	2.4/0.038	–	–
AT1G66090	Disease resistance protein (TIR-NBS class)		2.5/0.033	–	3.1/0.019	7.9/0.035
AT1G72920	Disease resistance protein (TIR-NBS class)		2.5/0.031	–	–	–
AT2G32140	Disease resistance protein (TIR class)		2.1/0.006	–	–	–
AT3G04220	Disease resistance protein (TIR-NBS-LRR class)		–	2.6/0.033	–	–
AT3G05370	Disease resistance family protein		2/0.040	–	2.3/0.011	–
AT3G48090	Disease resistance protein EDS1	EDS1	2.8/0.016	–	3.3/0.019	–
AT5G22690	Disease resistance protein (TIR-NBS-LRR class)		2.5/0.040	–	3.3/0.007	–
AT5G41740	Disease resistance protein (TIR-NBS-LRR class)		–	3/0.026	2.2/0.026	–

(Continued)

Table 1. (continued).

Arabidopsis Genome Initiative	Description	Name	NLP$_{Pp}$		flg22	
			1 h	4 h	1 h	4 h
Pathogenesis/Defense-Related Genes						
AT1G02360	Chitinase		10.8/0.024	15.2/0.019	20.9/0.019	18.8/0.005
AT2G43570	Chitinase		–	14.6/0.025	–	–
AT2G43590	Chitinase		6.8/0.045	21.9/0.021	7/0.025	–
AT3G47540	Chitinase		2.2/0.044	–	–	–
AT3G54420	Class IV chitinase (CHIV)	At EP3	–	5.6/0.013	–	23.5/0.002
AT4G01700	Chitinase		4.5/0.010	5/0.013	7.9/0.020	24.8/0.019
AT3G21230	4-Coumarate–CoA ligase/synthase	4CL	–	5/0.042	2.2/0.010	8.6/0.046
AT3G21240	4-Coumarate–CoA ligase/synthase 2	4CL2	–	2.6/0.036	3.2/0.030	–
AT1G65690	Harpin-induced protein-related/HIN1-related	HIN1-like	6.8/0.028	13.8/0.020	9.7/0.027	–
AT2G35980	Harpin-induced family protein (YLS9)/HIN1 family protein	HIN1	6.5/0.006	105/0.019	–	–
AT2G37040	Phe ammonia lyase 1	PAL1	–	3.9/0.038	–	6.5/0.013
AT1G80820	Cinnamoyl-CoA reductase	CCR2	3.4/0.017	–	6/0.007	–
AT5G14700	Cinnamoyl-CoA reductase-related		–	2.8/0.012	5.3/0.005	–
AT1G33960	Avirulence-responsive protein	AIG1	–	6.4/0.044	–	–
AT3G28930	avrRpt2-induced AIG2 protein	AIG2	–	3/0.021	–	–
AT4G39030	Enhanced disease susceptibility 5, SA-induction deficient 1	EDS5/SID1	–	4.4/0.029	–	–
AT1G74710	Isochorismate synthase/mutase	ICS (SID2)	–	5.4/0.028	–	–
AT3G26830	Cytochrome P450 CYP71B15	PAD3	–	45.8/0.025	–	–
AT5G05730	Anthranilate synthase, α-subunit, component I-1	ASA1	–	4/0.029	–	–
AT3G54640	Trp synthase, α-subunit	TSA1	–	3/0.038	–	–
AT4G39950	Cytochrome P450 79B2, putative	CYP79B2	–	4.9/0.045	–	–
AT3G45640	MAPK	MPK3	2.1/0.031	–	3.6/0.007	–
AT1G01560	MAPK	MPK11	3.8/0.012	–	5.6/0.004	–
AT2G26560	Patatin	PLP2	12.8/0.048	–	21.9/0.040	–
AT3G49120	Peroxidase	Perx34	2/0.037	3/0.020	–	2.1/0.036
AT4G11850	Phospholipase D γ 1	PLDγ	2.8/0.020	2.5/0.022	4.1/0.026	–
AT5G06860	Polygalacturonase inhibiting protein 1	PGIP1	–	2.9/0.029	–	5.7/0.013
AT4G12500	Protease inhibitor/seed storage/lipid transfer protein		–	6.6/0.046	–	144/0.037
AT3G22600	Protease inhibitor/seed storage/lipid transfer protein		5,6/0,024	60.8/0.013	–	2.4/0.045
AT5G47910	Respiratory burst oxidase protein D/NADPH oxidase	RbohD	2,4/0,008	2.4/0.020	2/0.024	–
AT1G64060	Respiratory burst oxidase protein F/NADPH oxidase	RbohF	–	2.1/0.031	–	–
AT3G06300	Oxidoreductase, 2OG-Fe(II) oxygenase		–	2.1/0.024	–	2.9/0.025
AT3G08710	Thioredoxin		2.3/0.023	–	2.4/0.012	–
AT1G62300	WRKY family transcription factor 6	WRKY6	4.5/0.016	5.3/0.022	6.7/0.015	5.7/0.008
AT1G80840	WRKY family transcription factor 40	WRKY40	2.8/0.046	4.5/0.022	3.4/0.007	–
AT2G23320	WRKY family transcription factor 15	WRKY15	2/0.032	3.2/0.026	3/0.005	5.2/0.046
AT2G24570	WRKY family transcription factor 17	WRKY17	3.7/0.015	3.6/0.019	8.5/0.026	20.6/0.015
AT2G38470	WRKY family transcription factor 33	WRKY33	2.4/0.017	5.3/0.020	2.6/0.007	–
AT2G46400	WRKY family transcription factor 46	WRKY46	–	3.6/0.038	–	4.3/0.040
AT4G18170	WRKY family transcription factor 28	WRKY28	2.7/0.050	6.8/0.032	6.3/0.044	7.7/0.020
AT4G24240	WRKY family transcription factor 7	WRKY7	–	2.3/0.020	3.5/0.009	13.8/0.029
AT4G31800	WRKY family transcription factor 18	WRKY18	–	2.6/0.042	–	–
AT5G24110	WRKY family transcription factor 30	WRKY30	–	13/0.026	–	–
AT5G46350	WRKY family transcription factor 8	WRKY8	–	9.5/0.019	–	6.1/0.0003
AT5G49520	WRKY family transcription factor 48	WRKY48	–	2.6/0.045	–	12.1/0.012
Hormone Signaling						
AT2G37040	Phe ammonia lyase 1	PAL1	–	3.9/0.038	–	6.5/0.013
AT4G39030	Enhanced disease susceptibility 5, SA induction deficient 1	EDS5/SID1	–	4.4/0.029	–	–
AT1G74710	Isochorismate synthase/mutase (ICS; EDS16)	ICS/SID2	–	5.4/0.028	–	–
AT1G01480	1-Aminocyclopropane-1-carboxylate synthase 2	ACC1, ACS2	2.8/0.005	–	4.4/0.006	–

(Continued)

Table 1. (continued).

Arabidopsis Genome Initiative	Description	Name	NLP_{Pp}		*flg22*	
			1 h	4 h	1 h	4 h
AT1G05010	1-Aminocyclopropane-1-carboxylate oxidase (ACO)	EAT1	–	2.1/0.025	–	–
AT4G26200	1-Aminocyclopropane-1-carboxylate synthase 7	ACS7	11.2/0.044	–	–	–
AT4G11280	1-Aminocyclopropane-1-carboxylate synthase 6	ACS6	–	5.8/0.028	–	2.8/0.013
AT1G05710	Ethylene-responsive protein		–	3.7/0.025	–	3.4/0.042
AT1G09740	Ethylene-responsive protein		–	2.5/0.020	–	–
AT5G47230	Ethylene-responsive element binding factor 5	ERF5	2.4/0.03	3/0.038	3.3/0.022	–
AT5G54510	Auxin-responsive GH3 protein	DFL-1	–	4.6/0.027	–	4.2/0.025

Average relative values from three independent experiments of NLP_{Pp} and flg22-treated samples compared with respective control samples and adjusted P values derived from one-way ANOVA analysis combined with a Benjamini and Hochberg false discovery rate calculation are given. Expression changes of less than twofold between treatment and control are indicated (–).

Arabidopsis is affected by the presence of NLP_{Ps} (NLP from *Phytophthora sojae*), surface-sterilized seeds were germinated on solid half-strength Murashige and Skoog (MS) medium supplemented with increasing concentrations of the purified recombinant protein. As shown in Figure 3, seedling root growth and vigor were significantly reduced at NLP_{Ps} concentrations of 0.1 μg/mL (4 nM). Germination and growth were completely inhibited at concentrations of 100 μg/mL or greater (Figure 3A), and root necrosis and macroscopic cell death could be observed similar to that reported recently on Nep1-treated seedlings (Bae et al., 2006). By contrast, seedling germination and development on half-strenth MS supplemented with heat-denatured NLP_{Ps} was normal relative to that observed on half-strenth MS alone (Figure 3C). The previous description of a naturally occurring flg22-insensitive *Arabidopsis* ecotype (Gomez-Gomez and Boller, 2000) prompted us to compare the responses of 17 different *Arabidopsis* ecotypes when germinated and grown in the presence of 2.0 μg/mL NLP_{Ps}. Each of the 17 ecotypes exhibited reduced growth and vigor. None of the selected subspecies appeared to be more or less sensitive toward 2.0 μg/mL NLP_{Ps} on a comparative basis (Figure 3B). Altogether, NLP_{Ps} negatively affects *Arabidopsis* seedling growth and development similar to flg22, but no evidence for genetic variation in this response was found among the *Arabidopsis* ecotypes tested.

The Physiological and Molecular Basis of NLP-Induced Plant Cell Death

Incompatible plant–pathogen interactions are often associated with HR PCD, while cell death in compatible interactions is a consequence of successful infection of host plants by necrotizing pathogens that commonly use toxins to kill their hosts (Greenberg and Yao, 2004). Although NLPs from various sources were shown to trigger cell death in dicot plants, the molecular basis of this response has not been fully explored. To further characterize NLP_{Pp}-induced cell death, we tested whether active plant metabolism is required for this type of cell death to occur. For this purpose, we chose to work on tobacco (*Nicotiana tabacum*) because this offered the opportunity to compare NLP_{Pp}-induced cell death with that caused by another oomycete-derived, cell

death–inducing elicitor, the elicitin β-megaspermin (Baillieul et al., 2003). As shown in Figure 4, the coinfiltration of leaves with elicitor and inhibitors of DNA transcription (α-amanitin) or protein biosynthesis (cycloheximide) completely abolished lesion formation caused by either elicitor. Likewise, LaCl$_3$, a nonspecific Ca^{2+} channel inhibitor, blocked NLP_{Pp} and β-megaspermin–induced cell death. Taken together, our findings suggest that NLP_{Pp}-induced cell death requires active host cellular metabolism.

Toxin-induced plant cell death and AVR/R protein–mediated cell death each have been described to be light dependent (Asai et al., 2000; Chivasa et al., 2005; Manning and Ciuffetti, 2005; Chandra-Shekara et al., 2006). We therefore investigated whether NLP_{Pp}-induced lesion formation would be affected by light. In initial experiments, infiltrations into tobacco leaves were performed in daylight, and plants were then transferred to darkness. Under these conditions, the NLP_{Pp} lesions were indistinguishable from those observed on plants kept in light (data not shown). Subsequently, we performed infiltrations in the dark, which resulted in weaker and delayed lesion development. Preconditioning the plants in darkness was necessary to eliminate lesion development entirely. Thus, when plants were kept in the dark for 30 min before infiltration of NLP_{Pp}, then infiltrated in darkness and kept there for 24 h, no lesion formation could be observed (Figure 5). Likewise, β-megaspermin–induced cell death was completely abolished under these conditions. The light dependence of NLP_{Pp}-mediated lesion development was also tested in *Arabidopsis.* As shown in Figure 5, NLP_{Pp}-induced cell death was also light dependent in this species as was HR PCD in response to infection by avirulent *P. syringae* pv *tomato* strain DC3000/AvrRpm1. Thus, at least one step in NLP_{Pp}-induced cell death in plants appears to depend on light.

Caspases (Cys-containing Asp-specific proteases) are Cys proteases that represent a core execution switch for animal PCD (Evan et al., 1995). Plants appear to lack caspase genes homologous to those found in animals or yeast, but caspase-like activities in plants have been inferred from inhibitor studies or enzymatic assays (Lam and del Pozo, 2000; Greenberg and Yao, 2004; Lam, 2004). We have made use of several types of caspase-specific peptide inhibitors (Ac-YVAD-CHO for caspase-1,
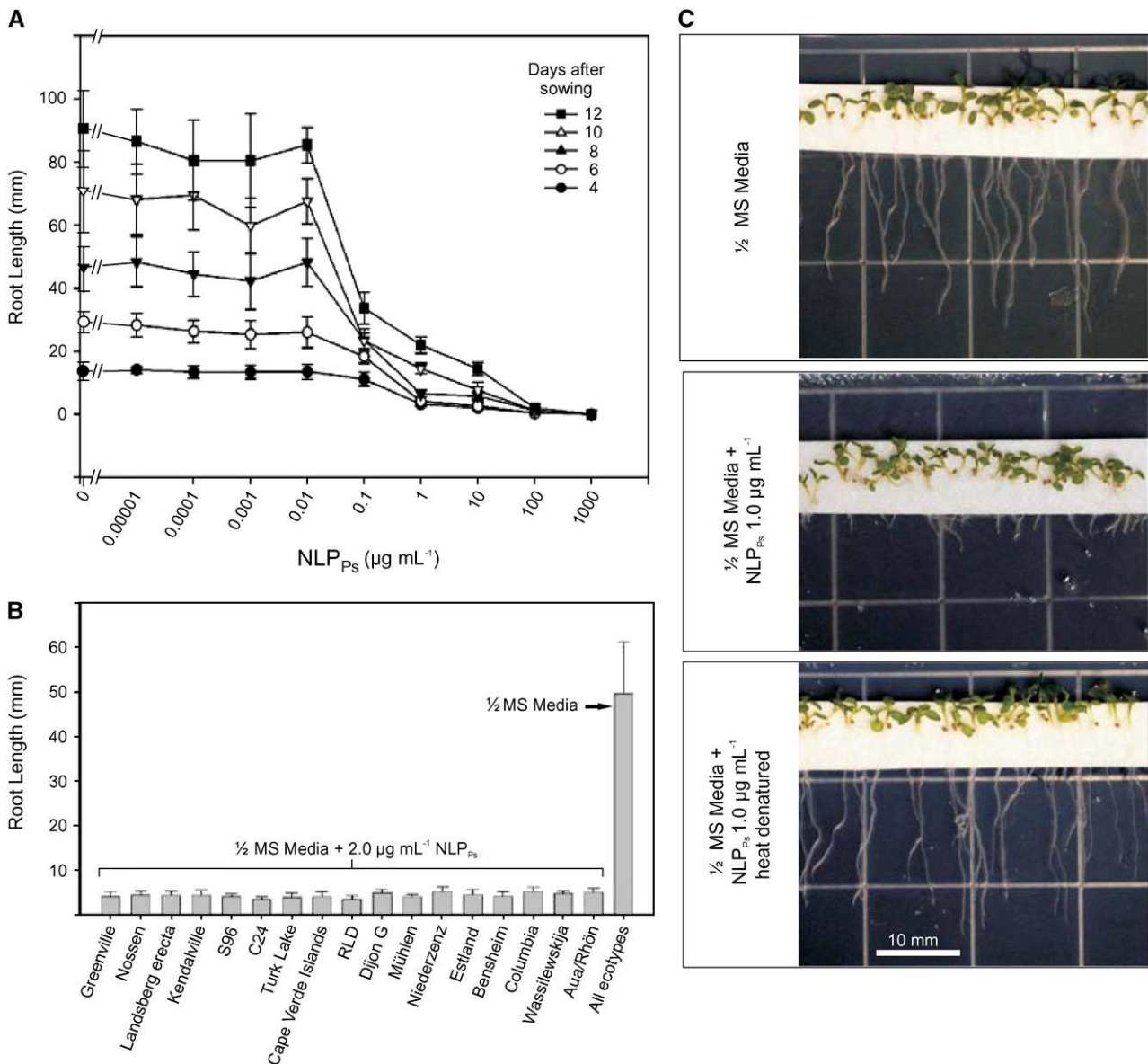
Figure 3. Germination of *Arabidopsis* Seedlings in the Presence of NLP$_{Ps}$.

(A) Seeds of *Arabidopsis* ecotype Col-0 were sown in sterile media containing a range of concentrations of NLP$_{Ps}$, and root lengths were measured at intervals as indicated. Shown are average values and SD from measurements of 10 to 20 plants (per treatment) from a representative experiment. The experiment was performed three times with similar results.

(B) Seeds of 17 *Arabidopsis* ecotypes were sown in sterile media, with and without added NLP$_{Ps}$, and root lengths were measured after 8 d. Shown are average values and SD from measurements of 10 to 20 plants (per ecotype) from a representative experiment. The experiment was performed three times with similar results.

(C) Seeds of *Arabidopsis* ecotype Col-0 were sown in sterile half-strength MS medium alone (top panel), on half-strength MS medium supplemented with 1.0 μg/mL NLP$_{Ps}$ (middle panel), or on half-strength MS medium containing 1.0 μg/mL heat-denatured NLP$_{Ps}$ (bottom panel). Photographs were taken 5 d after sowing.

Ac-DEVD-CHO for caspase-3, and zVAD-fmk for pan-caspases) to study a possible involvement of caspase-like proteases in NLP-induced cell death in tobacco plants (Hatsugai et al., 2004). Coinfiltration of either inhibitor with NLP$_{Pp}$ resulted in occurrence of lesions that were indistinguishable from those evoked by NLP$_{Pp}$ alone (Figure 6A). Thus, caspase-like activity sensitive to inhibitors of animal PCD appears not to be involved in NLP-mediated cell death. Similar results were obtained using Ac-VEID-FMK, an inhibitor of caspases-6 and -8 (data not shown). In control experiments, tobacco HR PCD triggered by infection with
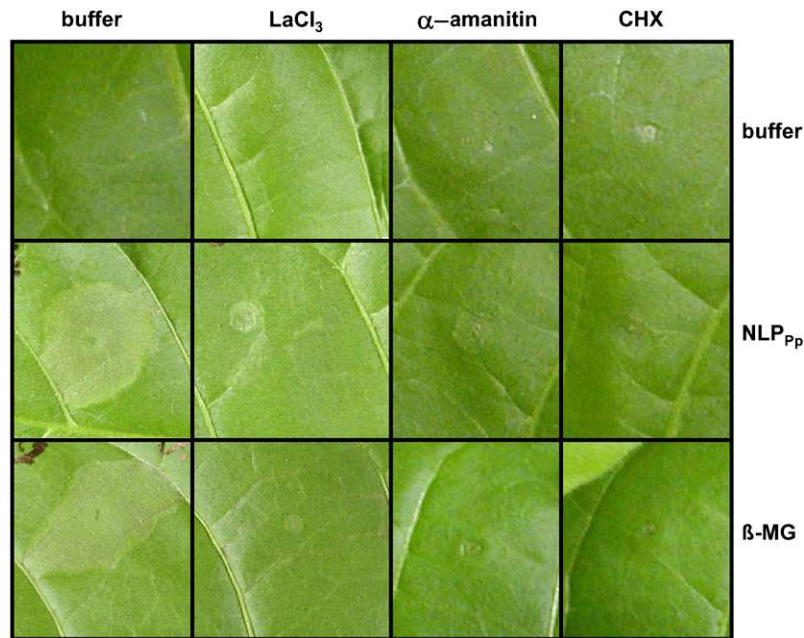
Figure 4. NLP-Induced Cell Death Requires Active Plant Metabolism.

Four-week-old tobacco plants were infiltrated either with the calcium channel blocker $LaCl_3$ (1 mM), with the DNA transcription inhibitor α-amanitin (100 μM), or the protein translation inhibitor cycloheximide (CHX; 100 μM) alone, in combination with buffer as control, or 1 μM NLP_{Pp} or 50 nM β-megaspermin (β-MG), respectively. PCD symptoms shown here were obtained after 2 d.

P. syringae pv *phaseolicola* was abolished by caspase inhibitors, as reported previously (del Pozo and Lam, 1998).

Mammalian Bax Inhibitor-1 (BI-1) is a known suppressor of apoptotic cell death in animal and yeast cells (Xu and Reed, 1998). Homologs of *BI-1* isolated from various plant species have been shown to act mechanistically similar to their animal counterparts (Lam, 2004). Recently, Watanabe and Lam (2006) reported the isolation of two *Arabidopsis* mutant lines that carried a T-DNA insertion in the At *BI1* gene (*atbi1-1* and *atbi1-2*). Gene inactivation resulted in accelerated progression of cell death upon treatment with the fungal toxin FB1. Administration of NLP_{Pp} caused lesion formation on the wild type and on both *atbi1* alleles tested (Figure 6B). The kinetics of lesion development and symptom severity were similar in wild-type and mutant lines, suggesting that BI-1 activity does not substantially contribute to the containment of NLP-induced lesions in *Arabidopsis.*

HR PCD in plants infected with avirulent pathogens requires SA. Likewise, FB1-induced cell death in *Arabidopsis* was shown to be dependent on SA (Asai et al., 2000). NLP_{Pp}-induced lesions, however, still developed in SA-deficient *nahG Arabidopsis* plants (Table 2), suggesting no SA requirement for this response. This is surprising because NLP_{Pp}-mediated expression of the *PR-1* gene was previously reported to be SA dependent (Fellbrich et al., 2002). Mutant plants impaired in NDR1 and PAD4 activity also developed wild-type-like lesions. Moreover, unlike FB1-induced cell death (Asai et al., 2000), NLP_{Pp}-triggered necrosis was observed on *coi1* and *ein2* genotypes, suggesting that

neither JA nor ethylene contributes to this phenotype. Kinetics of symptom development were indistinguishable from those observed on wild-type plants (data not shown).

SGT1b is a component of Skp1-Cullin-F-box protein ubiquitin ligases that target *Arabidopsis* regulatory proteins for degradation. Loss of *AtSgt1b* is associated with impaired plant cultivar-specific immunity (Azevedo et al., 2002). Moreover, lack of *Sgt1* in *Nicotiana benthamiana* resulted in inhibition of INF1 elicitin-mediated cell death (Peart et al., 2002). NLP_{Pp}-induced lesion formation, however, was not compromised in *sgt1b-1* plants or in *sgt1a-1* plants (Table 2), suggesting that it is either independent of SGT1 or that individual SGT1 isoforms may compensate for each other. The latter scenario is not testable because double knockout lines for both, *Atsgt1a* and *Atsgt1b*, are not viable (Hubert et al., 2003).

Two isoforms of *Arabidopsis* HSP90 (HSP90.1 and HSP90.2) are reported to compromise HR PCD in plant cultivar-specific immunity (Hubert et al., 2003; Takahashi et al., 2003). We tested two independent mutant alleles of each gene for impaired responsiveness to NLP_{Pp}. As shown in Table 2, we observed a partial reduction in NLP_{Pp}-mediated lesion formation on various HSP90 mutant alleles. Thus, HSP90 chaperone activity contributes to NLP_{Pp}-induced cell death. Plant cytosolic HSP90 also interacts with another chaperone-like protein, RAR1, which has been shown to play a critical role for the function of the *Arabidopsis* resistance proteins RPM1 and RPS2 (Hubert et al., 2003; Takahashi et al., 2003). However, *rar1* mutants did not exhibit altered NLP_{Pp} sensitivity (Table 2).
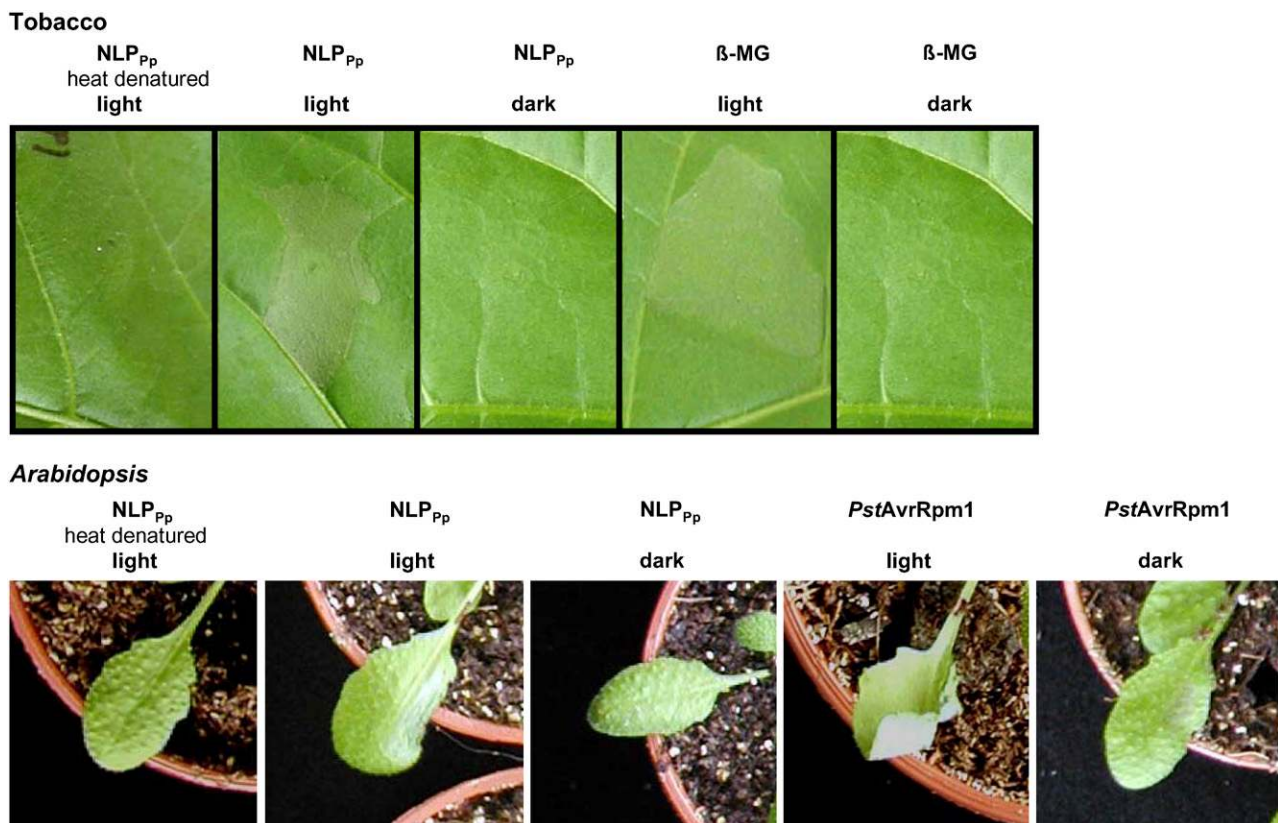
Tobacco

| NLP$_{Pp}$ heat denatured light | NLP$_{Pp}$ light | NLP$_{Pp}$ dark | ß-MG light | ß-MG dark |

Arabidopsis

| NLP$_{Pp}$ heat denatured light | NLP$_{Pp}$ light | NLP$_{Pp}$ dark | *Pst*AvrRpm1 light | *Pst*AvrRpm1 dark |

Figure 5. Light Dependence of NLP$_{Pp}$-Induced Cell Death.

Five-week-old tobacco (top panel) or *Arabidopsis* plants (bottom panel) were treated with 1 μM NLP$_{Pp}$, 1 μM heat-denatured NLP$_{Pp}$, 50 nM β-megaspermin (β-MG), or 5 × 10⁶ colony-forming units/mL *P. syringae* pv *tomato* strain DC3000/AvrRpm1 (PstAvrRpm1) under normal light conditions or 30 min upon transfer into the dark as indicated. PCD symptoms shown here were obtained after 2 d.

Sensitivity to NLP Is Restricted to Dicotyledonous Plant Cells

The apparent universal sensitivity of dicot plants to NLPs contrasts with the apparent insensitivity of monocot plants (Pemberton and Salmond, 2004; Gijzen and Nürnberger, 2006). Such an activity spectrum is unprecedented among known elicitors, including PAMPs, but is similar to that reported for host nonselective toxins, such as fusicoccin or FB1. It is also known that an NLP gene from *Vibrio pommerensis* maps to a genomic region that is indispensable for bacterial virulence and hemolysis of animal erythrocytes, perhaps pointing to an even larger range of cell types that are susceptible to NLPs (Jores et al., 2003). In contrast with PAMPs that bind to plant plasma membrane protein receptors, toxins may interact with host membranes in different ways. For example, CryA-type bacterial toxins (*Bacillus thuringiensis* toxin) act as membrane-disrupting cytolysins on insect or nematode cells upon docking to specific glycolipid plasma membrane constituents (Griffitts et al., 2005). To explore the interaction of NLP with phospholipid bilayers in greater detail, we tested living and synthetic membrane systems for susceptibility to this protein. In the first set of experiments, we attempted to clarify if NLP sensitivity is indeed restricted to dicot plant cells or, alternatively,

whether NLP treatment would destabilize phospholipid membrane systems in general but would leave monocot membranes intact due to some unknown counteractive measure. NLP concentrations similar to or higher than those reported to cause cell death in dicot cells were used. As shown in Table 3, addition of NLP to monolayers of human fibroblasts (line GM5756) or African green monkey kidney-derived COS-7 cells did not significantly increase cell mortality. This effect could be observed independent of the culture media that were used to grow these cell layers. A possible cell type–specific NLP sensitivity of animal cells was tested by supplementing sheep erythrocytes for up to 24 h with 1 μM NLP$_{Pp}$. However, at no time point did hemolysis caused by NLP$_{Pp}$ exceed that observed in control treatments (Table 3). Moreover, a possible Ca²⁺ requirement for NLP-induced erythrocyte death similar to that described for some bacterial cytolysins could not be demonstrated. Similarly, membranes of lower eukaryotes proved insensitive to NLP, as both *Pichia pastoris* cells and spheroplasts derived thereof survived treatment with this protein (Table 3). Likewise, the moss *Physcomitrella patens* was tested for NLP sensitivity. Moss cultures were grown either on solid medium or in liquid culture supplemented with 2 μM NLP$_{Pp}$ or with heat-inactivated NLP$_{Pp}$ as control. Under no circumstance was viability of the culture (Table 3) affected by
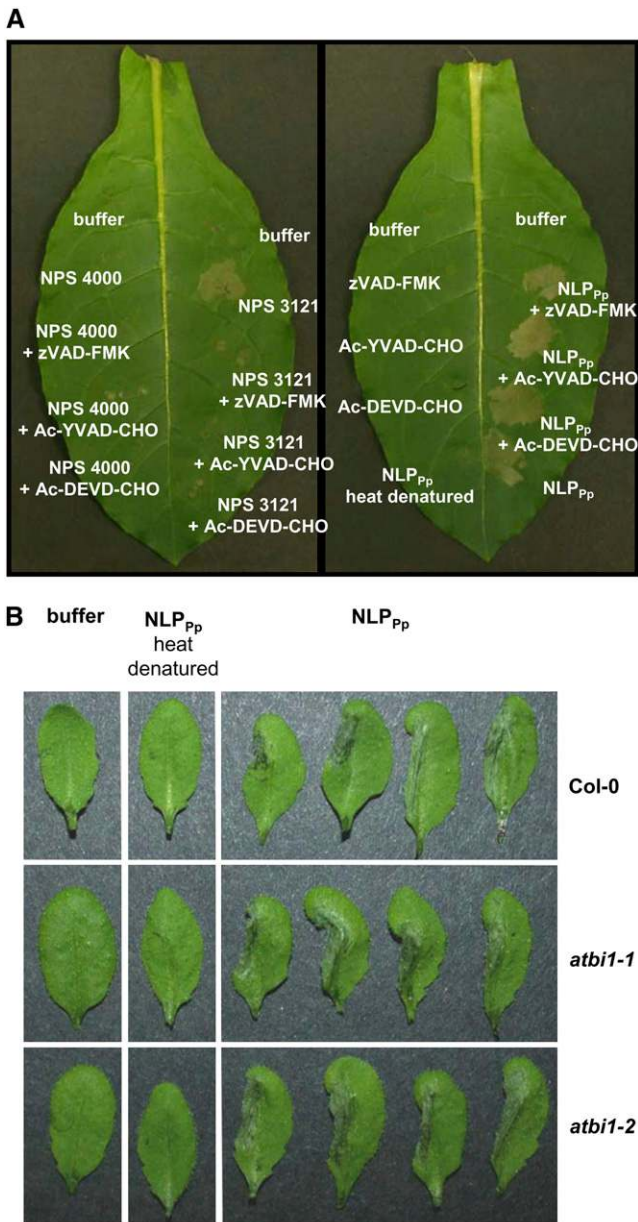
Figure 6. NLP-Induced PCD Is Independent of Caspase and Bax Inhibitor Activity.

(A) Tobacco leaves were infiltrated with 4 μM NLP$_{Pp}$ or *P. syringae* pv *phaseolicola* strains NPS4000 (PCD-noninducing strain) or NSP3121 (PCD-inducing strain) in the presence or absence of 100 μM of the caspase inhibitors Ac-YVAD-CHO, Ac-DEVD-CHO, or zVAD-FMK. Plants were kept at room temperature under continuous illumination.
(B) Five-week-old *Arabidopsis* Col-0, *atbi1-1*, or *atbi1-2* mutant plants were treated with 4 μM NLP$_{Pp}$, 4 μM heat-denatured NLP$_{Pp}$, or buffer as control.
Photographs in **(A)** and **(B)** were taken 24 h after infiltration.

NLP treatment nor was spore germination rate and differentiation affected (data not shown).

Experiments that demonstrated the insensitivity of monocots to NLPs were invariably performed by infiltration of the protein into leaf tissues or by droplet or spray application. To exclude the possibility that application conditions accounted for the virtual NLP insensitivity of monocot plant cells and to explore whether NLP sensitivity required an intact plant cell wall, monocot and dicot plant cell cultures and protoplasts were tested. As shown before, cell suspensions derived from the dicot plants *Arabidopsis* or parsley (*Petroselinum crispum*) were sensitive to NLP, whereas cell cultures of maize (*Zea mays*) proved insensitive to NLP treatment (Table 3). Strikingly, a similar result was obtained from experiments performed with protoplasts derived from *Arabidopsis*, parsley, or maize (Table 3, Figure 7), indicating that monocot plant cells are indeed fully insensitive to NLPs and that NLP sensitivity of dicot plant cells does not require the presence of the cell wall.

NLP Interacts with a Target Site That Is Unique to the Extracytoplasmic Side of Dicot Plant Plasma Membranes

Triggers of plant immune responses, such as PAMPs or endogenous elicitors, are recognized through binding to plant plasma membrane receptors (Nürnberger et al., 2004; Zipfel and Felix, 2005). The supposed NLP$_{Pp}$ affinity constant is ~10 nM, as deduced from the EC$_{50}$ = 8.5 nM for NLP$_{Pp}$-induced phytoalexin production in parsley (Fellbrich et al., 2002). However, receptor–ligand interaction studies or chemical cross-linking assays performed with various radioactively labeled NLP$_{Pp}$ preparations

Table 2. Mutational Analysis of NLP-Induced Cell Death

Arabidopsis Genotype	Cell Death Index
Col-0	1.64 ± 0.10
Ler-0	1.86 ± 0.14
nahG	1.77 ± 0.08
ndr1-1	1.81 ± 0.16
pad4-1	1.61 ± 0.17
coi1-1	1.33 ± 0.12
ein2-1	1.53 ± 0.17
sgt1a-1	1.83 ± 0.23
sgt1b-1	1.44 ± 0.20
rar1-10	1.83 ± 0.16
Col-0	2.00 ± 0.00
hsp90.1-1 (SALK 075596)	0.85 ± 0.05
hsp90.1-2 (SALK 007614)	0.89 ± 0.16
hsp90.2-3 (*lra2-3*)	1.00 ± 0.27
hsp90.2-5 (SALK 058553)	1.11 ± 0.08

Five-week-old *Arabidopsis* Col-0 wild type or mutant plants were infiltrated with 1 μM NLP$_{Pp}$ or GST as control (Fellbrich et al., 2002). PCD symptom development was scored 24 h after treatment and cell death indices calculated as described in Methods. Data shown in the lower part of the table represent experiments that were conducted independently of those shown in the top part. Therefore, a new set of controls (Col-0) is provided. Cell death indices were calculated as described in Materials. GST control treatments did not result in cell death. Thus, no average and SD values are given.

Table 3. Sensitivity to NLP Is Restricted to Dicotyledonous Plant Cells

Cell Type	NLP Concentration	Survivors Relative to Control (%) (±SD)
COS-7		
(DMEM)	1 μM NLP$_{Pp}$	57.5 ± 0.5
(Quantum 333)	1 μM NLP$_{Pp}$	85.5 ± 6.5
Human fibroblasts (GM5756)		
(DMEM)	1 μM NLP$_{Pp}$	85.5 ± 7.5
(Quantum 333)	1 μM NLP$_{Pp}$	120.5 ± 17.5
Sheep erythrocytes (PBS)	1 μM NLP$_{Pp}$	102.3 ± 4.7
− Ca^{2+}	2 μM NLP$_{Pya}$	97.7 ± 2.9
Sheep erythrocytes (PBS)	1 μM NLP$_{Ps}$	98.4 ± 5.7
+ Ca^{2+}	2 μM NLP$_{Pya}$	96.4 ± 12.1
P. pastoris spheroplasts	1 μM NLP$_{Ps}$	86.2 ± 9.5
	2 μM NLP$_{Pya}$	52.0 ± 4.3
P. patens	2 μM NLP$_{Pp}$	100.7 ± 11.8
Maize cell culture	0.1 μM NLP$_{Pya}$	112.3 ± 2.6
	1 μM NLP$_{Pya}$	91.1 ± 2.8
Arabidopsis cell culture	1 μM NLP$_{Pya}$	40.3 ± 4.6
Parsley cell culture	1 μM NLP$_{Pya}$	7.2 ± 0.8
Maize protoplasts	0.1 μM NLP$_{Pp}$	88.3 ± 11.8
Arabidopsis protoplasts	1 μM NLP$_{Pp}$	89.7 ± 8.4
	0.1 μM NLP$_{Pya}$	102.2 ± 15.7
	1 μM NLP$_{Pya}$	97.2 ± 7.5
	0.1 μM NLP$_{Pp}$	5.7 ± 2.4
	1 μM NLP$_{Pp}$	3.1 ± 1.6
	0.1 μM NLP$_{Pya}$	4.2 ± 0.9
	1 μM NLP$_{Pya}$	1.0 ± 0.9
Parsley protoplasts	0.1 μM NLP$_{Pp}$	4.4 ± 0.8
	1 μM NLP$_{Pp}$	2.2 ± 1.0
	0.1 μM NLP$_{Pya}$	2.2 ± 0.9
	1 μM NLP$_{Pya}$	0.6 ± 0.6

Various cell types were treated with different NLP preparations at the concentrations indicated. Cell death rates were determined at times and using protocols described in Methods. Values represent average values ± SD.

failed to detect a high-affinity binding site on parsley microsomal membranes (data not shown). Therefore, other scenarios of signal perception may apply in the case of NLPs. As some cytolytic toxins that cause inflammatory responses and PCD in animal cells were shown to bind to lipid components of host membranes (Parker and Feil, 2005), we tested whether NLP$_{Pp}$ displayed affinity to lipid membranes in vitro. Silica beads coated with a single phospholipid bilayer (TRANSIL) were incubated with NLP$_{Pp}$, subsequently collected by centrifugation, and analyzed by SDS-PAGE (Figure 8A). The majority of NLP$_{Pp}$ was found to be lipid associated, whereas the supernatant was depleted of the protein. Variations in the phospholipid composition (ratio between the two major phospholipid species in eukaryotic membranes, 1,2-diacyl-*sn*-glycero-3-phosphocholine/POPC and 1,2-diacyl-sn-glycero-3-phosphoethanolamine/POPE) had no apparent impact on the phase distribution of NLP$_{Pp}$. Importantly, BSA, a major lipid and fatty acid carrier protein of the blood circulatory system, bound very little to TRANSIL beads, suggesting that NLPs display a marked affinity to lipid membranes.

Ionophores, such as amphotericin B, have been shown to trigger the activation of plant defense–associated responses in

various systems in a non-receptor-mediated manner (Jabs et al., 1997). To test whether NLP$_{Pp}$ exerts ionophore activity that may cause activation of plant defense, including PCD, we added the protein to synthetic bilayer liposomes that were loaded with the cation-sensitive fluorescent dye Sodium Green. As shown in Figure 8B, no NLP$_{Pp}$-mediated Na$^+$ influx and subsequent fluorescence emission was observed, suggesting that the protein itself did not form cation-conducting pores in the membrane. Moreover, no membrane collapse similar to that evoked by 0.1% Triton X-100 was observed (data not shown), suggesting that the protein does not randomly disrupt phospholipid bilayers. Importantly, the bacterial effector protein HrpZ$_{Psph}$ from *P. syringae* pv *phaseolicola* mediated ion pore formation as shown previously (Lee et al., 2001). HrpZ$_{Psph}$ and related bacterial effectors form ion-conducting pores not only in artificial membranes but also in biological membranes, such as the plasma membrane of *Xenopus laevis* oocytes (our unpublished data; Racape et al., 2005). However, NLP$_{Pya}$ proved insufficient to generate any ion currents in this system (Figure 8C), suggesting that it did not directly affect membrane integrity through intrinsic ionophore activity.

NLPs are secretory proteins with a likely exposure to the apoplastic side of the plant plasma membrane during infection.
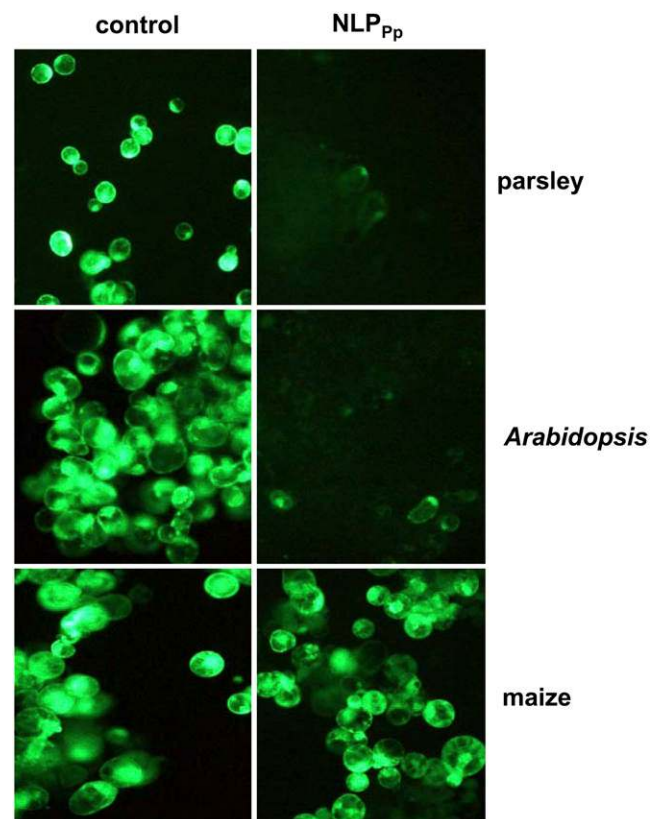

Figure 7. NLP-Induced Cell Death in Dicot Plants Does Not Require Intact Plant Cell Walls.

Parsley, *Arabidopsis*, or maize protoplasts (5 × 10^5/mL) prepared from cultured cells were treated with 1 μM NLP$_{Pp}$ for 24 h, and viability staining was performed as described in Methods.
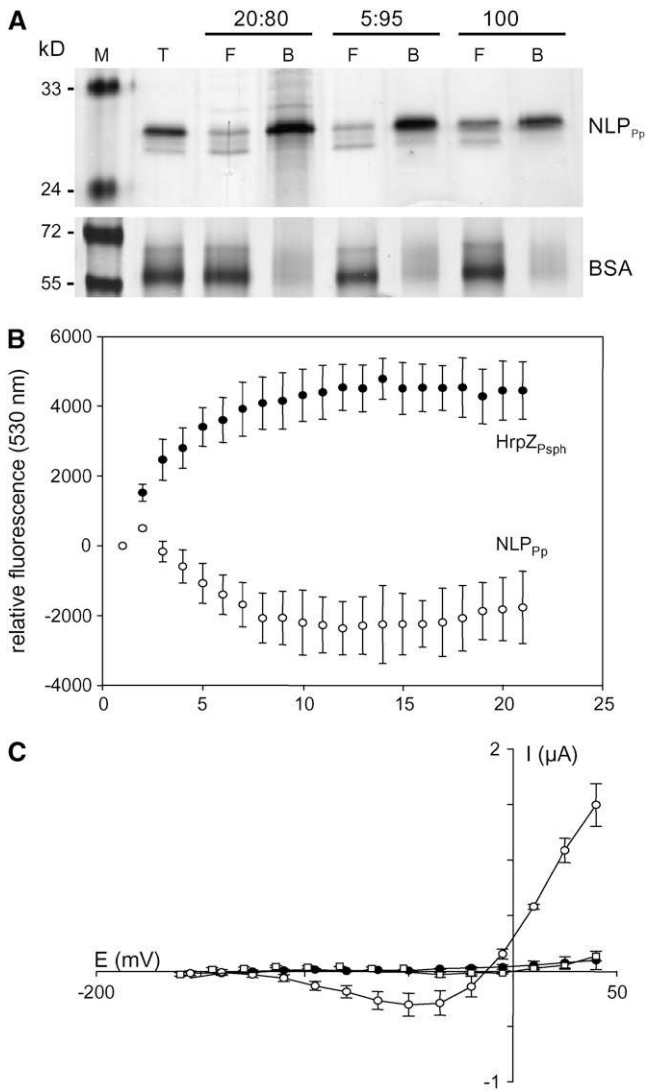
Figure 8. NLPs Possess Binding Affinity to Phospholipid Bilayers but Do Not Show Pore-Forming Activity on Artificial and Biological Membranes.

(A) TRANSIL beads coated with POPE/POPC (20:80), POPE/POPC (5:95), or POPC alone were incubated for 1 h with 1 μM NLP$_{Pp}$ (total protein [T]). After separation of lipid-bound (B) from free unbound material (F), proteins were analyzed by SDS-PAGE and silver staining.
(B) Na$^+$ influx into Sodium Green–filled liposomes. Sodium-mediated fluorescence was measured without protein and in the presence of 1 μM NLP$_{Pp}$ (open symbols) or 1 μM HrpZ$_{Psph}$ (closed symbols). Fluorescence values obtained without protein were subtracted from values obtained in the presence of either protein. Values given represent the means ± SD from assays performed in triplicate.
(C) Two-electrode voltage clamp measurements on *X. laevis* oocytes. The current/voltage plots obtained before and after the application of 1 μM NLP$_{Pya}$ (open squares and closed circles, respectively) or 1 μM HrpZ$_{Psph}$ (open circles) are shown. Steady state currents were measured following 4-s pulses. The results presented are representative of those obtained in three experiments ±SD.

Thus, interaction of NLPs at the extracytoplasmic side rather than the cytoplasmic side of the host plasma membrane can be predicted to occur. To test a possible side-specific activity of NLPs at the plant plasma membrane, three independent experimental systems were used to express the protein with (+SP) or without (−SP) a signal peptide. As shown in Figure 9, transient biolistic cotransformation of *Arabidopsis* leaves with the NLP$_{Ps}$(−SP) gene and the reporter gene β-glucuronidase (GUS) resulted in detectable GUS activity. By contrast, no GUS activity could be observed in experiments when NLP$_{Ps}$(+SP) was expressed. This finding indicates that NLP$_{Ps}$(+SP)-induced cell death occurred prior to GUS expression. In a similar experimental setup, cobombardment of soybean leaves with the same cassette or of sugar beet (*Beta vulgaris*) leaves with a NLP$_{Pp}$(−SP)/ *Renilla reniformis* luciferase cassette yielded significant reporter enzyme activity, while luciferase activity remained at control levels upon expression of NLP$_{Pp}$(+SP) fused to a plant signal peptide (see Supplemental Figure 3 online). In summary, delivery to the apoplastic side of the plant cell surface is a requirement for NLP-induced cell death. Altogether, our findings suggest that NLP sensitivity is not a consequence of nonspecific membrane disruption but requires a specific target site that is unique to the extracytoplasmic side of dicot plant cell membranes.

DISCUSSION

Taxonomic Distribution and Activity Pattern of NLPs Favor a Role as Nonself Recognition Determinants in Plant Immunity

We have retrieved a total of 44 NLP-encoding genes representing 22 microbial species from public databases (Figure 1; see Supplemental Figure 1 online). NLP sequences are distinguished by an unusually wide distribution across microbial taxa (bacteria, fungi, and oomycetes) but are absent from the genomes of plants and animals. It is thus reasonable to assume that NLPs support a microbial lifestyle. More than 70% of the NLP sequences currently known originate from plant pathogenic microorganisms that rely on hemibiotrophic or necrotrophic nutrition, suggesting that these proteins may facilitate various forms of heterotrophic growth in plants in particular. Recently, whole-genome sequencing was completed for the two oomycete phytopathogens *P. sojae* and *Phytophthora ramorum* (http://www.jgi.doe.gov) as well as for the two fungal plant pathogens *Magnaporthe grisea* and *Fusarium graminearum* (*Gibberella zeae*). Comparative genomic analyses revealed that the *Phytophthora* NLP families are much larger in size (50 to 60 loci in each species) than those in fungi (four loci in each species), perhaps pointing to a special role for these proteins in oomycete plant pathogens. While the reason for the evolutionary expansion and diversification of the NLP family in *Phytophthora* species is yet to be resolved, it is apparent that NLPs represent a molecular pattern that is common in organisms of this genus.

The taxonomic distribution pattern of NLP raises concerns regarding the physiological role of these proteins during infection. The cytolytic activities of NLPs, their contribution to fungal
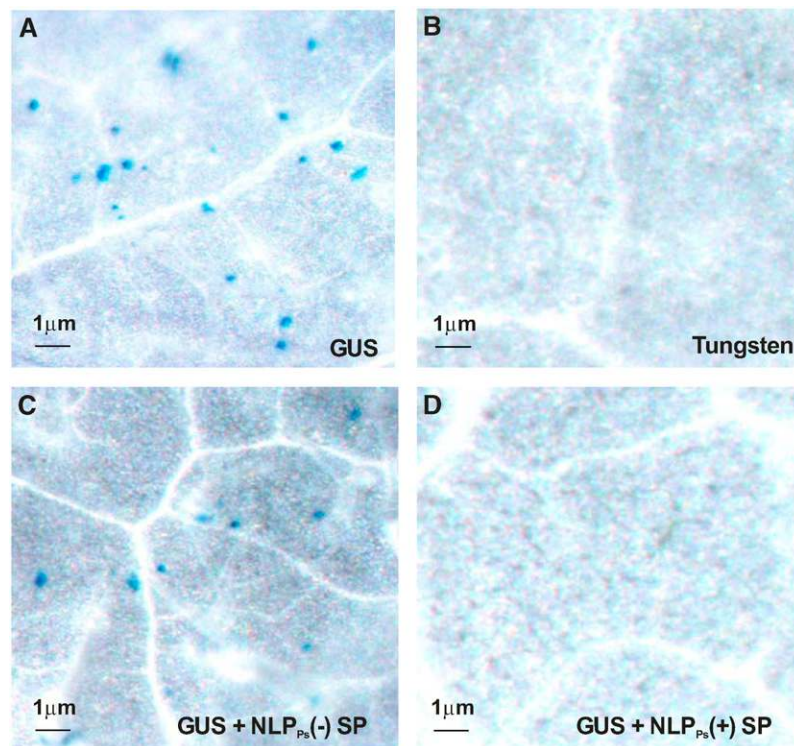
Figure 9. NLP-Induced PCD Requires Delivery to and Recognition at the Extracytoplasmic Side of Dicotyledonous Plant Cells.

Activity of NLP$_{Ps}$ in *Arabidopsis* leaves as determined by a cobombardment and transient expression assay. The photographs show *Arabidopsis* leaves after bombardment with tungsten beads and histochemical staining for GUS activity, performed as described in Methods. The tungsten beads were treated as follows: **(A)**, coated with pFF19G containing a GUS expression cassette; **(B)**, uncoated tungsten beads alone; **(C)**, coated with pFF19G (GUS) plus a pFF19 construct encoding NLP$_{Ps}$ lacking a signal peptide [NLP$_{Ps}$(-)SP]; **(D)**, coated with pFF19G (GUS) plus a pFF19 construct encoding NLP$_{Ps}$, including the complete open reading frame with the native signal peptide [NLP$_{Ps}$(+)SP].

and bacterial virulence, and induced NLP$_{Ps}$ transcript and protein accumulation during transition from biotrophic to necrotrophic growth seem to support a role as toxin-like effectors during plant infection (Pemberton and Salmond, 2004; Gijzen and Nürnberger, 2006). Moreover, conditional expression of the NLP$_{Ps}$ gene in *Arabidopsis* resulted in rapid wilting and cell death (E. Huitema and S. Kamoun, unpublished data), and transformation of an avirulent *E. carotovora* strain that lacked NLP$_{Ec}$ with NLP$_{Pp}$ rescued virulence on potato tubers (M. Pirhonen, unpublished data), which indicates that the protein is toxic to plant cells. Our current finding that highly conserved NLP sequences occur predominantly in organisms that live at least partially heterotrophically also supports an important physiological role of these proteins. It is thus conceivable that NLPs may contribute to a heterotrophic lifestyle by either directly killing the host and/or by facilitating access to nutrient sources through breaking down biological membranes. Moreover, several studies, including our recent work, have now shown that NLP sensitivity is restricted to dicot plant cells in a non-species-specific manner. Such a relatively wide activity spectrum is another feature that is characteristic of toxins. Likewise, the ability to trigger defense responses in a large number of plant species also distinguishes NLPs from other stimuli, such as PAMPs, AVR effectors, or endogenous elicitors. In most cases, these signals exert plant immune-stimulating activities in only a limited number of plant species or plant cultivars.

However, the broad taxonomic distribution of NLPs, in particular their occurrence in both prokaryotic and eukaryotic species, is quite unusual for known microbial phytotoxins. The production of phytotoxins is often restricted to a narrow range of microbial species (van't Slot and Knogge, 2002; Wolpert et al., 2002); therefore, NLPs seem to represent an unprecedented case. Thus, alternative molecular functions of NLPs may be considered. Several publications reported that NLP activity is heat-labile and is not restricted to a certain domain of the protein, suggesting that NLPs may possess enzymatic activity (Veit et al., 2001; Fellbrich et al., 2002; Qutob et al., 2002). Database analyses with intact or partial NLP sequences, however, did not yield any meaningful alignment with enzyme-encoding nucleotide sequences (data not shown). Moreover, heat labile and tertiary structure-dependent activities are also characteristics of proteinaceous toxins that are known to possess cytolytic activities on animal cells (Parker and Feil, 2005). Taken together, we propose that NLPs are virulence-promoting microbial effectors that exhibit toxin-like characteristics, but we admit that a classification of NLPs as genuine toxins requires a detailed

understanding of their molecular mode of action and the identification of host cell targets.

NLPs Trigger a Complex Immune Response in *Arabidopsis*

A broad taxonomic distribution and a wide variety of sensitive plant species are appropriate characteristics of nonself recognition determinants in plant–pathogen interactions. In this report, we have comprehensively characterized the immune response of one particular plant, *Arabidopsis*, to NLP_{Pp}. Results from this study and from previous work allow us to conclude that NLPs evoke a complex immune response. This response includes MAPK activation, production of NO, ethylene, camalexin, and callose, and extensive reprogramming of the transcriptome. Cell death and tissue necrosis terminates this massive defense response. The effects of NLPs resemble those triggered by the genuine PAMP flg22, with the exception that flg22 does not induce necrosis formation. In particular, very early responses, such as the production of NO and posttranslational activation of MAPK activity, are indistinguishable upon stimulation with NLPs or flg22. This is important because these responses occur at time points (within 30 min after stimulation) that clearly precede the onset of NLP-induced necrosis, suggesting that cell death may not be the cause for the induction of plant defense responses. The most compelling evidence that immediate and early plant responses to NLP and flg22 are comparable originates from whole-genome array-based transcriptome analyses. Large qualitative and quantitative overlaps were found in gene sets whose expression was altered upon application of either elicitor (Figures 2D and 2E). Gene sets whose expression is upregulated by either stimulus could be grouped into very similar functional categories. Intriguingly, genes implicated in pathogen recognition, such as receptor-like kinases, resistance signaling (disease resistance proteins, WRKY transcription factors, and hormone biosynthesis), and plant defense execution (PR proteins) were found to be coexpressed, suggesting that both signals are perceived as equivalent determinants of microbial nonself by the plant and similarly trigger activation of the plant surveillance system.

Overall, the microarray data indicate that NLPs and flagellin have a similar potential to trigger vital plant immune responses and may thus play similar roles in plant–microbe interactions, insofar as activation of plant defense is concerned. This view is further supported by experiments that showed that phytopathogenic bacteria-derived virulence factors suppress plant defense gene expression triggered by NLP_{Pp} or flg22, respectively, and thereby intercept with plant immunity (He et al., 2006).

Several recent studies have addressed the impact of pathogen-derived toxins on the plant transcriptome or on plant defense gene expression. For example, a comprehensive array experiment conducted on *Arabidopsis* plants treated with the cell death–inducing AAL toxin reported upregulation of oxidative stress and ethylene-responsive genes (Gechev et al., 2004), some of which were found to be upregulated in our experiment as well. Moreover, WRKY18 transcript accumulation in *Arabidopsis* in response to foliar application of Nep1 was reported (Keates et al., 2003). This finding was confirmed in our experiments, as was the accumulation of transcripts encoding ACS in *Arabidopsis* plants that were treated with *Verticillium dahliae* NLP_{Vd} (Wang et al., 2004).

A prime difference between flg22 and NLP is the ability of the latter to cause cell death. Thus, some of the genes that were exclusively found to be expressed in NLP-treated plants may found the basis for this particular plant response. We compared the transcriptome response of NLP_{Pp} with that caused by flg22 as well as with that caused by another cell death–inducing agent, FB1. Interestingly, among the 320 genes that were specifically induced by FB1, but not by flg22, we found no genes for which expression was also triggered by NLP_{Pp}. Thus, different cell death–inducing agents appear to have rather different effects on the *Arabidopsis* transcriptome. Another promising experimental approach lies in searching for NLP-insensitive *Arabidopsis* mutants. This strategy may take advantage of NLP-based inhibition of seedling vigor and root growth. Such a strategy has been pursued to identify *Arabidopsis* mutants impaired in toxin FB1 sensitivity (Stone et al., 2000) as well as the flagellin receptor FLS2 (Gomez-Gomez and Boller, 2000).

In the past, NLPs have been synonymously called elicitors, PAMPs, and toxins since they share properties with each of these classes of molecules. Classifying a particular molecule as an elicitor, PAMP, or a toxin can become a nebulous exercise due to the overlapping definitions (van't Slot and Knogge, 2002; Gijzen and Nürnberger, 2006). Individual pathogen-secreted effectors may also play multiple roles that simultaneously place them in different categories. The categories and terms themselves are somewhat arbitrary and have been extemporaneously defined. Nonetheless, the vocabulary is entrenched and does provide a common set of terms for the conceptualization of certain molecules. Identifying a molecule as an elicitor, PAMP, or a toxin when it is appropriate may also be more informative than simply evading the issue and referring to it as an effector. In our view, NLPs constitute toxin-like molecules that likely act as positive virulence factors during attempted infection but may also act as elicitors that mediate activation of the plant immune system. In contrast with PAMPs, which are defined as constitutive and evolutionarily conserved building blocks of microbial surfaces that directly bind to plant pattern recognition receptors, NLPs are considered to be part of the inducible microbial weaponry whose mode of interaction with plant cells remains to be elucidated.

NLPs Induce a Distinct Type of PCD

Both the HR (resistance-associated) and susceptible (disease-associated) cell death exhibit apoptotic features, such as DNA laddering, chromatin condensation, and terminal deoxynucleotidyl transferase-mediated dUTP nick end labeling. Thus, both types of cell death are likely to share common mechanistic elements (Greenberg and Yao, 2004). Interestingly, NLP_{Pya}- or NLP_{Vd}-induced plant cell death is accompanied by fragmentation of nuclear DNA (Veit et al., 2001; Wang et al., 2004) that resembles that caused by the cytolytic phytotoxin, thaxtomin A from *Streptomyces scabiei* (Duval et al., 2005). We found that NLP-induced PCD is light dependent and requires active plant metabolism. These characteristics are shared by AVR effector-mediated HR PCD and by PCD triggered by oomycete-derived elicitins. Interestingly, FB1 or *Pyrenophora tritici-repentis* ToxA toxin-induced PCD has also been reported to depend on

light (Chivasa et al., 2005; Manning and Ciuffetti, 2005), and thaxtomin-induced PCD requires plant transcriptional and translational activities (Duval et al., 2005). However, unlike PCD responses triggered by AVR effectors or the toxin FB1, NLP-induced PCD does not show any requirement for the plant defense–associated hormones SA, JA, or ethylene (Asai et al., 2000; Pieterse and Van Loon, 2004). Even more surprisingly, NLP-induced cell death proved to be independent of SGT1/SGT1b activity. Functionality of SGT1/SGT1b was proposed to be crucial to any type of HR PCD in response to AVR effectors or the elicitin INF1 (Azevedo et al., 2002; Peart et al., 2002). Likewise, no evidence that would support a role of caspase or BAX/BI activity in NLP-induced PCD was obtained. However, partial inhibition of NLP-induced PCD in *HSP90.1* or *HSP90.2* knockout plants that is qualitatively similar to that reported for AvrRpt2 or AvrRpm1-induced PCD in *Arabidopsis* (Hubert et al., 2003; Takahashi et al., 2003) suggests that chaperone activity promotes NLP PCD. This is also in agreement with reports on elicitin INF1-induced cell death in *N. benthamiana* that was shown to be dependent on HSP90 and HSP70 activity (Kanzaki et al., 2003). In summary, NLP-induced cell death exhibits features that are both shared with and distinct from other known types of PCD. A major distinction between AVR effector and NLP-induced PCD is the apparent lack of requirement for SGT1b and SA. Importantly, NLP_{Pp}-induced *PR1* gene expression in *Arabidopsis* was previously shown to require SA (Fellbrich et al., 2002), suggesting that different signal transduction pathways exist for activation of different facets of plant defense. This concept of different signaling cascades is also in agreement with our data that show that NLP_{Pp}-induced phytoalexin production, but not PCD in parsley, is dependent on an NLP_{Pp}-induced oxidative burst (Fellbrich et al., 2002). A similarly complex scenario was reported from tobacco cells that were treated with the elicitin INF1. In this system, separate signaling pathways mediating PCD, *PR* gene expression, and ROS production were described (Sasabe et al., 2000). Likewise, Pep-13–induced HR, but not *PR* gene expression, requires SA in potato (Halim et al., 2004).

Recently, fusaric acid (FA)–induced PCD in *Arabidopsis* was reported to require 100-fold higher concentrations than those used to trigger defense-associated responses, such as camalexin production (Bouizgarne et al., 2006). This surprising finding indicates that sublethal FA doses are sufficient to trigger innate immune responses but not PCD. In addition, FA-induced PCD appears to constitute a disease symptom (likely due to the cytolytic activity of FA) rather than a typical defense response. Strikingly, many bacteria-derived toxins that exert cytolytic activity on animal cells are known to trigger innate immune responses at sublethal doses (Srivastava et al., 2005; Ratner et al., 2006). Although this aspect of NLP activity deserves attention and needs to be re-explored in more detail, our findings argue against such a mode of action. NLP_{Pp} concentrations required for NLP-induced PCD and phytoalexin production in cultured parsley cells were found to be comparable (Fellbrich et al., 2002). Likewise, NLP_{Vd} concentrations required to induce PCD and phytoalexin production in cotton (*Gossypium hirsutum*) differed slightly but were in the same order of magnitude (Wang et al., 2004). NLP-induced PCD may thus constitute an element of the plant innate surveillance system that is deliberately activated by necrotrophic pathogens that strive to kill their hosts.

Activity of NLPs on Dicot Cells Is Plasma Membrane Side Specific

We have demonstrated that sensitivity to NLPs is restricted to dicot plants and cannot be found in other plant families or in animal cells. Thus, the previously reported NLP stability of monocot membranes is not a peculiarity of these systems. These findings suggest a dicot-specific perception system or target for NLPs. As we failed to identify a proteinaceous plant NLP_{Pp} binding site by classical biochemical methods that have previously proved successful in identifying the PAMP binding site in other plant systems (Nürnberger et al., 2004), we addressed the question whether there were any specific requirements for recognition of NLPs. We could show that NLP perception was independent of the cell wall. Moreover, NLPs may not possess intrinsic ionophore activity that has previously been reported to activate individual plant defense responses (Jabs et al., 1997). Most importantly, NLP-induced cell death occurred only when the protein was targeted to the apoplastic side of dicot cells, indicating that there is plasma membrane side specificity. Despite that NLPs appear to possess a general affinity toward phospholipid bilayers, specific components that are unique to the apoplastic surface of dicot plasma membranes appear to provide a target for NLP. A prevailing theory is that PAMPs or endogenous elicitors are supposed to act through plasma membrane receptors (Gomez-Gomez and Boller, 2000; Nürnberger et al., 2004; Zipfel and Felix, 2005; Zipfel et al., 2006). In contrast with these signals that are selectively perceived by a limited number of plant species, NLPs are apparently recognized by all dicot plants. Thus, perception or target sites that are conserved among all dicots are likely to mediate NLP recognition. Such a wide activity/recognition spectrum is reminiscent of toxin action. It is thus conceivable that NLPs may bind to their virulence targets and subsequently activate a plant immune response.

Our understanding of PCD in plant cells is incomplete, but evidence to date indicates that there are multiple pathways and host cellular targets that may initiate this process. Host-selective toxins, such as the ToxA protein from *P. tritici-repentis* and the host nonselective, sphingoid-like natural product FB1 from *Fusarium moniliforme*, both appear to trigger defense responses and PCD but via different routes. ToxA must be internalized by the cell to activate PCD, while FB1 works on the outside by depleting extracellular ATP (Chivasa et al., 2005; Manning and Ciuffetti, 2005). Fusicoccin is a nonselective toxin that binds to a complex of the membrane H^+-ATPase associated with a 14-3-3 protein (Wurtele et al., 2003), stimulates the membrane H^+-ATPase, and causes stomatal opening and wilting but does not rapidly activate PCD. The host-selective peptide toxin victorin is known to bind to the P-protein component of the mitochondrial matrix-located Gly decarboxylase complex, but recently it has been demonstrated that the toxin interacts with a cell surface mediator and triggers defense responses and PCD well before binding to the P-protein (Wolpert et al., 2002; Tada et al., 2005). Proteinaceous toxins produced by *Alternaria* spp are

host selective and cause rapid necrosis and host cell death in susceptible plants (Quayyum et al., 2003; Oka et al., 2005). Overall, these chosen examples serve to illustrate the variety of known toxins and the apparent diversity in their mechanism of action and spectrum of activity. The phenomenon of toxin-induced innate immune responses is also known from animal cells. Multiple bacteria-derived proteinaceous toxins have been shown to target specific cell surface structures prior to exerting cytolytic activities (Parker and Feil, 2005). For example, the Cry family of *B. thuringiensis* insecticidal proteins requires membrane glycolipid receptors for toxin action (Griffitts et al., 2005). Importantly, toxin-induced MAPK pathways and large alterations in the host transcriptome precede PCD and are accounted for as toxin-induced defense (Huffman et al., 2004).

The examples are also useful for comparison. Reflecting on the effects of NLPs upon plant cells and their contribution to pathogen virulence, it is clear that these proteins can be considered toxins. This may be the most parsimonious interpretation of NLP activity, but it is a view that is likely to be incomplete on its own. Dual roles for molecules as both elicitors and toxins are well known in plant pathogens. The emergence of the so-called guard hypothesis to account for many gene-for-gene interactions (Chisholm et al., 2006) also belies earlier and simpler theories and provides a warning that parsimony in nature can follow unexpected paths.

Crucial for our understanding of NLPs is to learn more about the mechanism of action and mode of perception by the plant immune system. Evidence presented here, and in previous work, has demonstrated that NLPs have a natural affinity for lipid bilayers and that their activity and specificity do not require the presence of a cell wall. The necessity for signal peptides for activity of ectopically expressed NLPs is another important finding. Together, these results point to a target site-of-action on the outer surface of dicotyledonous plant cell plasma membranes. The identity of this target and the nature of its interaction with NLPs are outstanding questions. Other important aspects of NLP action on plants, such as the genetic determination of the cell death response as well as the elucidation of the precise virulence-associated function of these proteins, need to be addressed. Answers to these questions are necessary to clarify the role of NLPs in pathogen–host interactions and will lead to a better and more sophisticated understanding of toxin action in plants.

METHODS

All *Arabidopsis thaliana* materials used were in the Col-0 background if not otherwise indicated. *Arabidopsis* and tobacco plants (*Nicotiana tabacum* cv Samsun NN) were grown on soil (Fellbrich et al., 2002). Soybean seeds of *Glycine max* cv Harosoy (Agriculture and Agri-Food Canada) were planted in 10-cm pots containing soil-less mix (Pro-Mix BX; Premier Horticulture). Plants were grown for ∼2 weeks in a controlled growth chamber with supplementary light to give a 16-h photoperiod with 22°C day and 20°C night temperatures. Sugar beet (*Beta vulgaris*) plants (genotype 6B2840; KWS SAAT) were grown as described (Schmidt et al., 2004). *Arabidopsis* Col-0 *nahG* (Syngenta), *coi1-1*, *ndr1-1*, *pad4-1*, *sgt1a*, *sgt1b*, L*er*-0 *rar1-10* (Jane Parker and Paul Schulze-Lefert, MPIZ Köln, Germany), *ein2-1* (ABRC), *hsp90.1-1*, *hsp90.1-2*, *hsp90.2-5* (SALK collection), and hsp90.2-3 (Jeff Dangl, Chapel Hill, NC) were obtained from

the sources indicated. Dark-grown cell cultures of parsley (*Petroselinum crispum*), *Arabidopsis* L*er*-0, and maize (*Zea mays*) were maintained and protoplasts prepared thereof as described (Hart et al., 1993; Nürnberger et al., 1994; Dettmer et al., 2006). *Physcomitrella patens* cultures were grown in modified Knop medium containing 250 mg/L KH_2PO_4, 250 mg/L $MgSO_4 \times 7H_2O$, 250 mg/L KCl, 1 g/L $Ca(NO_3)_2 \times 4H_2O$, and 12.5 mg/L $FeSO_4 \times 7H_2O$, pH 5.8 as liquid culture or on modified Knop medium solidified with 8 g/L agar. Cultures were grown in a light chamber (25°C, 70 μE m^{-2} s^{-1} light intensity) in a 16-h-light/8-h-dark cycle. Human fibroblasts (line GM5756; Dodt et al., 1995) and COS-7 cells were grown as monolayers on Dulbecco's modified Eagle's medium (DMEM) supplemented with 4.5 g/L glucose, 10% fetal calf serum, 1 mg/mL geniticin, and 2 mM glutamine or on Quantum 333 medium (PAA Laboratories) at 37°C under a 5 to 8.5% CO_2 atmosphere. Sheep erythrocytes (Fiebig-Nährstofftechnik) and *Pichia pastoris* spheroplasts (Invitrogen) were prepared and stored according to the supplier's instructions. *Pseudomonas syringae* pv *tomato* strain DC3000/AvrRpm1 and *P. syringae* pv *phaseolicola* strains NPS4000 or NSP3121 were grown as described (del Pozo and Lam, 1998; Hubert et al., 2003).

Elicitor Preparation

Recombinant NLP_{Pp} or NLP_{Pya} were produced as described (Veit et al., 2001; Fellbrich et al., 2002). Recombinant NLP_{Ps} was produced in *Escherichia coli* strain BL21(DE3) transformed with pET28a-PsojNIP (Qutob et al., 2002). One hundred microliters of an overnight culture were transferred into Luria-Bertani medium containing 50 $\mu g/mL$ kanamycin, grown at 37°C to an $OD_{600} = 0.5$, supplemented with 1 mM isopropyl-D-thiogalactoside, and cultivated overnight at 37°C under constant agitation. Bacterial pellets were harvested by centrifugation (10,000*g*, 15 min, 4°C) and resuspended in Bugbuster protein extraction reagent (Novagen) at a final concentration of 0.2 g/mL. Suspensions supplemented with 25 units/mL Benzonase Nuclease (Novagen) were kept at room temperature for 20 min, and inclusion bodies (IBs) were recovered by centrifugation (16,000*g*, 15 min, 4°C). Lysozyme (200 $\mu g/$ mL) was added to pellets redissolved in the same volume of extraction buffer for 5 min. After addition of 6 volumes of 1/10 diluted extraction buffer, IBs were harvested by centrifugation as before, washed repeatedly, and stored in 10 mM Tris-HCl, pH 8.0. For solubilization and refolding, IBs were resuspended in extraction buffer supplemented with 1% SDS and kept at room temperature for 90 min. Supernatants collected by centrifugation (16,000*g*, 15 min, 4°C) were dialyzed at 15°C successively against 0.8%, 0.6%, 0.4%, 0.2%, and 0.1% SDS, and, finally, against 10 mM Tris, pH 8.0, and stored at 4°C prior to use. Protein concentrations were determined using Bradford reagent, and concentrated stock solutions were prepared. Heat inactivation of NLP was achieved by incubation at 95°C for 15 min. Recombinant $HrpZ_{Psph}$ was prepared, and flg22 was chemically synthesized as described (Lee et al., 2001; Fellbrich et al., 2002). Purified β-megaspermin was a kind gift of Serge Kauffmann (Centre National de la Recherche Scientifique).

Arabidopsis Growth Inhibition Assays

Half-strength MS medium with 10 g/L sucrose was prepared, the pH was adjusted to 5.7, and agar was added to 0.8% (w/v). The medium was autoclaved and allowed to cool to 50°C. Aliquots were decanted into 50 mL conical tubes and mixed with recombinant NLP stock solutions (0.1 to 1.0 mL, previously filter sterilized). This medium was poured into square Petri dishes. Sterile filter paper strips (Whatman No. 1) were placed across the solid agar plates near one edge. Seeds were surface sterilized, suspended (2000 to 3000 seeds/mL) in half-strength MS medium with sucrose and 0.15% agar, and dispensed with a pipette onto the filter strips. The plates were propped up in a nearly vertical position with the filter

strips and seeds along the top edge, in a controlled environment (25°C, 70 μE m^{-2} s^{-1} light intensity, 16-h-light/8-h-dark cycle).

Elicitation of Plant Defense Responses

NLPs dissolved in water were infiltrated abaxially into leaf tissue using needleless 1-mL plastic syringes (Roth). Routinely, infiltrations were performed on 5-week-old *Arabidopsis* or 4-week-old tobacco plants. Leaves were harvested at indicated time points to monitor symptom development. Bacterial infection assays were performed as described (del Pozo and Lam, 1998; Hubert et al., 2003). NO synthesis in *Arabidopsis* cell suspensions and camalexin production in plants were quantified as described (Glawischnig et al., 2004; Zeidler et al., 2004). Samples were analyzed by reverse phase HPLC (LiChroCART 250-4, RP-18, 5 μm; Merck) (1 mL·min^{-1}; methanol/H$_2$O [1:1] for 2 min, followed by a 10 min linear gradient to 100% methanol, followed by 3 min at 100% methanol). The peak at 10.6 min was identified as camalexin by comparison with authentic standard with respect to retention time and UV spectrum (photodiode array detector; Dionex) and quantified using a Shimadzu F-10AXL fluorescence detector (318-nm excitation; 370-nm emission) and by UV absorption at 318 nm. For MAPK activity assays, infiltrated plant material was harvested and used for total protein extraction in 25 mM Tris-HCl, pH 7.8, 75 mM NaCl, 15 mM EGTA, 15 mM glycerophosphate, 15 mM 4-nitrophenylpyrophosphate, 10 mM MgCl$_2$, 1 mM DTT, 1 mM NaF, 0.5 mM Na$_3$VO$_4$, 0.5 mM PMSF, 10 μg/mL leupeptin, 10 μg/mL aprotinin, and 0.1% Tween 20. Proteins were collected by centrifugation (23,000g, 10 min, 4°C), subjected to SDS-PAGE (20 μg protein/lane), and electrophoretically transferred (100 V, 1 h, 25 mM Tris-HCl, ph 8.3, 0.192 M glycine, and 20% methanol) to nitrocellulose membranes (Porablot NCL; Macherey-Nagel). After blocking in 20 mM Tris-HCl, pH 8.3, 150 mM NaCl, 0.1% Tween 20, and 5% dry milk (room temperature, 1 h), membranes were incubated overnight at 4°C with a 1:1000 dilution of Phospho-p44/42 MAP kinase antibody (Cell Signaling Technology) followed by an incubation with a 1:10,000 dilution of blotting grade affinity-purified goat-anti-rabbit IgG(H+L)-HRP conjugate (Bio-Rad). Immunodetection was performed using the ECL Plus chemiluminescence detection kit (GE Healthcare).

Plasmid Construction

To excise the signal peptide-encoding region from the NLP$_{Pp}$-coding sequence, a new translation start codon was introduced into the coding sequence of the NLP$_{Pp}$ gene in pGEX-5x-NLP$_{Pp}$ (Fellbrich et al., 2002). A 236-bp PCR product was amplified using primers 5′-GAAGGTCGTGG-GATCCCCGCCATGGACGTG-3′ and 5′-TGACTGCCGTATCCGGAGC-CCTTGCA-3′. *Bam*HI-*Kpn*I–digested PCR fragments were ligated into pGEX-5x-NLP$_{Pp}$ linearized with the same restrictases yielding pGEX-ATG-NLP$_{Pp}$. A 662-bp *Xho*I-*Nco*I fragment from pGEX-ATG-NLP$_{Pp}$ was fused to the 35S promoter-encoding sequence in pSH9 (Holtorf et al., 1995). The signal peptide-encoding sequence of the barley (*Hordeum vulgare*) α-amylase gene was amplified from pLys13 using the primers 5′-TACCGGGATCCCCCTCGAGGTCGACGA-3′ and 5′-TATGAATTCG-GACGCCAACCCGGCGAGAAGC-3′. A 122-bp *Bam*HI-*Eco*RI fragment of the PCR product was ligated into linearized pGEX-5x-NLP$_{Pp}$. A 734-bp *Xho*I-*Nco*I fragment of the resulting plasmid was fused to the 35S promoter-encoding sequence in pSH9 (Holtorf et al., 1995) (pGEX-SP-NLP$_{Pp}$). The identity of all constructs was confirmed by DNA sequencing.

Phylogenetic Analysis

Protein sequences deposited to GenBank were searched using the Conserved Domain Database to find matches to the NPP1 domain (pfam05630). This tool relies on the reverse position-specific BLAST algorithm to identify conserved domains in protein sequences (Marchler-Bauer et al., 2005). A total of 65 protein sequence hits to the NPP1 domain were returned. After correction for redundancy, 44 protein sequences containing an NPP1 domain were identified. These nonredundant sequences were further analyzed for phylogenetic and molecular evolutionary relationships using computer software (MEGA version 3.1; Kumar et al., 2004). Sequences were aligned using ClustalW, and an unrooted phylogram was made using the neighbor-joining method. A bootstrap consensus tree was drawn with branch values from 1000 replicates.

Cell Viability Assays

Plant cell and protoplast viability assays (5 × 10^5/mL) were performed as described (Veit et al., 2001; Fellbrich et al., 2002). Methods for the determination of *P. patens* viability (increase in culture dry weight over a 3-week growth period), spore germination rate, and differentiation are available at http://www.plant-biotech.net/ under the topic Moss Methods. Sheep erythrocytes were centrifuged (600g, 5 min, room temperature), washed three times in TBS (10 mM Tris-HCl, pH 7.2, and 140 mM NaCl), and resuspended at 1% (v/v) in TBS. NLP solutions were added to 1 mL erythrocytes (3 × 10^7) supplemented with or without 10 mM CaCl$_2$. Cells were smoothly agitated (37°C, 100 rpm), samples were collected after 1, 6, and 24 h, and cells harvested by centrifugation (600g, 10 min, room temperature). Hemoglobin release was monitored by quantifying absorbance of the supernatant at 542 nm. No hemolysis (blank) and full hemolysis controls comprised erythrocytes resuspended in TBS or in TBS and 0.5% SDS. Results are given as percentage of viable cells relative to the value of the blank control, set arbitrarily at 100%. *P. pastoris* spheroplasts were resuspended in CaS medium or CaSMD medium (Invitrogen) at a density of OD$_{600}$ = 1.0 (5 × 10^7 cells/mL). NLP solutions were added to 1 mL of spheroplasts, and suspensions were incubated at room temperature for 1 or 24 h. At these time points, 200 μL samples were subjected to quantification of absorbance at 600 nm. No lysis (blank) and full lysis controls comprised spheroplasts resuspended in CaS medium supplemented with 20 mM Tris HCl, pH 8.9, 1 mM GSH, 1 mM GSSG, and 1 mM EDTA or in CaS medium containing 10% SDS. Results are given as percentage of viable cells relative to the value of the blank control, set arbitrarily at 100%. For viability tests, fibroblast or COS-7 cells were separated from confluent growth plates by incubation in 0.05% trypsin/EDTA dissolved in Ca^{2+}/Mg^{2+}-free Hank's buffer (PAA Laboratories) and subsequently dissolved in fresh DMEM or Quantum 333 media. Fibroblasts (6 × 10^5/mL) or COS-7 (2 × 10^5/mL) were supplemented with NLP and kept for 28 h at 37°C under 5 to 8.5% CO$_2$ atmosphere. Prior to trypan blue viability staining, cells were trypsinized as before and counted as described (Dodt et al., 1995). The cell death index of intact *Arabidopsis* plants was determined on the basis of visual examination of lesion size 24 h after treatment (0, no lesions; 1, speckled lesions at inoculation sites; 2, confluent lesions at inoculation sites). Cell index values represent average numbers (±SD) obtained from 12 infiltrated leaves from each of two independent experiments.

Microarray Experiments

Microarray experiments performed on *Arabidopsis* Col-0 plants infiltrated with 1 μM NLP$_{Pp}$ or 1 μM flg22 were part of the AtGenExpress Initiative (http://www.arabidopsis.org/info/expression/ATGenExpress.jsp). Details for plant cultivation, infiltration, RNA preparation, array design, and data sets can be found in the AtGenExpress section at The Arabidopsis Information Resource (http://www.arabidopsis.org/servlets/TairObject?type=expression_setandid=1008080727). Affymetrix ATH1 high-density oligonucleotide gene arrays were used for triplicate hybridizations of each biological sample. Global analysis of temporal gene expression was performed by subjecting the absolute expression values for scaling using

Affymetrix MAS5.0 software. Scaled mean values of expression were imported into Genespring software (version 7.2; Agilent Technologies) using a gcRMA (Schmid et al., 2005) plug-in normalization tool prior to data analysis. Means of three replicate values for each data set were analyzed for stimulus-induced differential gene expression. Data sets with expression levels below 50 were excluded from comparative analyses (noise level of expression cutoff). Genes were considered as up- or downregulated if their mean expression levels deviated more than twofold from that of the nonelicited control samples. Statistical significance of gene expression was tested using a one-way ANOVA test combined with a Benjamini and Hochberg false discovery rate multiple correction algorithm (Genespring 7.2) with an adjusted P value < 0.05 set as cutoff.

Biolistic Transformations

Detached soybean leaves were surface-sterilized (40 s in 20% sodium hypochloride containing a few drops of surfactant Tween 20 and 1 to 3 s in 70% ethanol, followed by three rinses in sterile distilled water) prior to aseptic transfer adaxial side down on solid (0.8% [w/v] agar) MS induction media, pH 5.8 (Gibco) containing 0.1 mg/L α-naphthalene acetic acid, 1.0 mg/L benzyladenine, 100 mL B5 media, 750 mg/L CaCl$_2$, and 30 g/L sucrose. Two-week-old *Arabidopsis* Col-0 seedlings were transferred to fill a 3-cm-diameter circle at the center of a 60-mm Petri plate overlaid with a sheet of filter paper (Whatman No. 1) premoistened with 1.0 mL sterile water. All tissue samples were preincubated at 25°C, under fluorescent light (4000 lx) 24 h prior to biolistic transformation. Conditions for microprojectile transformation of leaves were as previously described, using expression vector pFF19 containing the GUS reporter gene (Qutob et al., 2002). Bombardments were performed with at least three independent DNA preparations with three sequential replica shots per DNA preparation. Histochemical localization of GUS expression was assayed as described (Qutob et al., 2002) with the modification that, following overnight incubation at 37°C, chlorophyll was cleared from leaf tissue with several washes in 70% (v/v) ethanol prior to examination by light microscopy. Biolistic transient expression assays with sugar beet leaves and luciferase activity measurements were performed as described (Schmidt et al., 2004) using the Bluescript derivate d35S:luc encoding the *Renilla reniformis* luciferase gene fused to a 35S promoter as a reporter for gene expression. Bombardments were performed with two independent DNA preparations with six sequential replica shots per DNA preparation.

Biochemical and Cell Physiological Assays

Phospholipid binding assays using lipid-coated silica beads (TRANSIL; Nimbus Biotechnology) were performed as described (Lee et al., 2001). Liposomes filled with the cation-sensitive fluorescent dye Sodium Green (Invitrogen) were obtained from Novosom. Ion pore formation experiments and patch-clamp analyses using *Xenopus laevis* oocytes were performed as described (Racape et al., 2005).

Supplemental Data

The following materials are available in the online version of this article.

Supplemental Figure 1. Alignment of 44 Different NLP Protein Sequences Using ClustalW.

Supplemental Figure 2. Taxonomic Distribution Pattern of NLP Sequences in Prokaryotes and Eukaryotes.

Supplemental Figure 3. NLP-Induced PCD Requires Delivery to and Recognition at the Extracytoplasmic Side of Dicotyledonous Plant Cells.

Supplemental Table 1. List of Genes That Are Significantly Induced upon NLP$_{Pp}$ Treatment (1 h).

Supplemental Table 2. List of Genes That Are Significantly Induced upon NLP$_{Pp}$ Treatment (4 h).

Supplemental Table 3. List of Genes That Are Significantly Induced upon flg22 Treatment (1 h).

Supplemental Table 4. List of Genes That Are Significantly Induced upon flg22 Treatment (4 h).

Supplemental Table 5. List of Genes That Are Coordinately and Significantly Induced upon Both NLP$_{Pp}$ and flg22 Treatment (1 and 4 h).

REFERENCES

Akira, S., Uematsu, S., and Takeuchi, O. (2006). Pathogen recognition and innate immunity. Cell **124,** 783–801.

Alfano, J.R., and Collmer, A. (2004). Type III secretion system effector proteins: Double agents in bacterial disease and plant defense. Annu. Rev. Phytopathol. **42,** 385–414.

Amsellem, Z., Cohen, B.A., and Gressel, J. (2002). Engineering hypervirulence in a mycoherbicidal fungus for efficient weed control. Nat. Biotechnol. **20,** 1035–1039.

Asai, T., Stone, J.M., Heard, J.E., Kovtun, Y., Yorgey, P., Sheen, J., and Ausubel, F.M. (2000). Fumonisin B1-induced cell death in *Arabidopsis* protoplasts requires jasmonate-, ethylene-, and salicylate-dependent signaling pathways. Plant Cell **12,** 1823–1836.

Asai, T., Tena, G., Plotnikova, J., Willmann, M.R., Chiu, W.L., Gomez-Gomez, L., Boller, T., Ausubel, F.M., and Sheen, J. (2002). MAP kinase signalling cascade in *Arabidopsis* innate immunity. Nature **415,** 977–983.

Ausubel, F.M. (2005). Are innate immune signaling pathways in plants and animals conserved? Nat. Immunol. **6,** 973–979.

Azevedo, C., Sadanandom, A., Kitagawa, K., Freialdenhoven, A., Shirasu, K., and Schulze-Lefert, P. (2002). The RAR1 interactor SGT1, an essential component of *R* gene-triggered disease resistance. Science **295,** 2073–2076.

Bae, H., Kim, M., Sicher, R., Bae, H.-J., and Bailey, B. (2006). Necrosis- and ethylene-inducing peptide from *Fusarium oxysporum* induces a complex cascade of transcripts associated with signal transduction and cell death in *Arabidopsis.* Plant Physiol. **141,** 1056–1067.

Bailey, B. (1995). Purification of a protein from culture filtrates of *Fusarium oxysporum* that induces ethylene and necrosis in leaves of *Erythroxylum coca.* Phytopathol. **85,** 1250–1255.

Baillieul, F., de Ruffray, P., and Kauffmann, S. (2003). Molecular cloning and biological activity of alpha-, beta-, and gamma-megaspermin, three elicitins secreted by *Phytophthora megasperma* H20. Plant Physiol. **131,** 155–166.

Bouizgarne, B., et al. (2006). Early physiological responses of *Arabidopsis thaliana* cells to fusaric acid: Toxic and signalling effects. New Phytol. **169,** 209–218.

Chandra-Shekara, A.C., Gupte, M., Navarre, D., Raina, S., Raina, R., Klessig, D., and Kachroo, P. (2006). Light-dependent hypersensitive response and resistance signaling against Turnip Crinkle Virus in *Arabidopsis.* Plant J. **45,** 320–334.

Chisholm, S.T., Coaker, G., Day, B., and Staskawicz, B.J. (2006). Host-microbe interactions: Shaping the evolution of the plant immune response. Cell **124,** 803–814.

Chivasa, S., Ndimba, B.K., Simon, W.J., Lindsey, K., and Slabas, A.R. (2005). Extracellular ATP functions as an endogenous external metabolite regulating plant cell viability. Plant Cell **17,** 3019–3034.

del Pozo, O., and Lam, E. (1998). Caspases and programmed cell death in the hypersensitive response of plants to pathogens. Curr. Biol. **8,** 1129–1132.

Dettmer, J., Hong-Hermesdorf, A., Stierhof, Y.D., and Schumacher, K. (2006). Vacuolar H$^+$-ATPase activity is required for endocytic and secretory trafficking in *Arabidopsis.* Plant Cell **18,** 715–730.

Dodt, G., Braverman, N., Wong, C., Moser, A., Moser, H.W., Watkins, P., Valle, D., and Gould, S.J. (1995). Mutations in the PTS1 receptor gene, PXR1, define complementation group 2 of the peroxisome biogenesis disorders. Nat. Genet. **9,** 115–125.

Duval, I., Brochu, V., Simard, M., Beaulieu, C., and Beaudoin, N. (2005). Thaxtomin A induces programmed cell death in *Arabidopsis thaliana* suspension-cultured cells. Planta **222,** 820–831.

Evan, G.I., Brown, L., Whyte, M., and Harrington, E. (1995). Apoptosis and the cell cycle. Curr. Opin. Cell Biol. **7,** 825–834.

Fellbrich, G., Romanski, A., Varet, A., Blume, B., Brunner, F., Engelhardt, S., Felix, G., Kemmerling, B., Krzymowska, M., and Nürnberger, T. (2002). NPP1, a *Phytophthora*-associated trigger of plant defense in parsley and *Arabidopsis.* Plant J. **32,** 375–390.

Gallucci, S., and Matzinger, P. (2001). Danger signals: SOS to the immune system. Curr. Opin. Immunol. **13,** 114–119.

Gechev, T.S., Gadjev, I.Z., and Hille, J. (2004). An extensive microarray analysis of AAL-toxin-induced cell death in *Arabidopsis thaliana* brings new insights into the complexity of programmed cell death in plants. Cell. Mol. Life Sci. **61,** 1185–1197.

Gijzen, M., and Nürnberger, T. (2006). Nep1-like proteins from plant pathogens: Recruitment and diversification of the NPP1 domain across taxa. Phytochemistry **67,** 1800–1807.

Glawischnig, E., Hansen, B.G., Olsen, C.E., and Halkier, B.A. (2004). Camalexin is synthesized from indole-3-acetaldoxime, a key branching point between primary and secondary metabolism in *Arabidopsis.* Proc. Natl. Acad. Sci. USA **101,** 8245–8250.

Glazebrook, J. (2005). Contrasting mechanisms of defense against biotrophic and necrotrophic pathogens. Annu. Rev. Phytopathol. **43,** 205–227.

Gomez-Gomez, L., and Boller, T. (2000). FLS2: An LRR receptor-like kinase involved in the perception of the bacterial elicitor flagellin in *Arabidopsis.* Mol. Cell **5,** 1003–1011.

Greenberg, J.T., and Yao, N. (2004). The role and regulation of programmed cell death in plant-pathogen interactions. Cell. Microbiol. **6,** 201–211.

Griffitts, J.S., Haslam, S.M., Yang, T., Garczynski, S.F., Mulloy, B., Morris, H., Cremer, P.S., Dell, A., Adang, M.J., and Aroian, R.V. (2005). Glycolipids as receptors for *Bacillus thuringiensis* crystal toxin. Science **307,** 922–925.

Halim, V., Hunger, A., Macioszek, V., Landgraf, P., Nürnberger, T., Scheel, D., and Rosahl, S. (2004). The oligopeptide elicitor pep-13 induces salicylic acid-dependent and -independent defense reactions in potato. Physiol. Mol. Plant Pathol. **64,** 311–318.

Hart, J., DiTomaso, J., and Kochian, L. (1993). Characterization of paraquat transport in protoplasts from maize (*Zea mays* L.) suspension cells. Plant Physiol. **103,** 963–969.

Hatsugai, N., Kuroyanagi, M., Yamada, K., Meshi, T., Tsuda, S., Kondo, M., Nishimura, M., and Hara-Nishimura, I. (2004). A plant vacuolar protease, VPE, mediates virus-induced hypersensitive cell death. Science **305,** 855–858.

He, P., Shan, L., Lin, N.-C., Martin, G., Kemmerling, B., Nürnberger, T., and Sheen, J. (2006). Specific bacterial suppressors of MAMP signaling upstream of MAPKKK in *Arabidopsis* innate immunity. Cell **125,** 563–575.

Holtorf, S., Apel, K., and Bohlmann, H. (1995). Comparison of different constitutive and inducible promoters for the overexpression of transgenes in *Arabidopsis thaliana.* Plant Mol. Biol. **29,** 637–646.

Hubert, D.A., Tornero, P., Belkhadir, Y., Krishna, P., Takahashi, A., Shirasu, K., and Dangl, J.L. (2003). Cytosolic HSP90 associates with and modulates the *Arabidopsis* RPM1 disease resistance protein. EMBO J. **22,** 5679–5689.

Huffman, D.L., Abrami, L., Sasik, R., Corbeil, J., van der Goot, F.G., and Aroian, R.V. (2004). Mitogen-activated protein kinase pathways defend against bacterial pore-forming toxins. Proc. Natl. Acad. Sci. USA **101,** 10995–11000.

Jabs, T., Tschöpe, M., Colling, C., Hahlbrock, K., and Scheel, D. (1997). Elicitor-stimulated ion fluxes and O_2^- from the oxidative burst are essential components in triggering defense gene activation and phytoalexin synthesis in parsley. Proc. Natl. Acad. Sci. USA **94,** 4800–4805.

Jores, J., Appel, B., and Lewin, A. (2003). Cloning and molecular characterization of a unique hemolysin gene of *Vibrio pommerensis* sp. *nov.*: Development of a DNA probe for the detection of the hemolysin gene and its use in identification of related *Vibrio* spp. from the Baltic Sea. FEMS Microbiol. Lett. **229,** 223–229.

Kamoun, S. (2006). A catalogue of the effector secretome of plant pathogenic oomycetes. Annu. Rev. Phytopathol. **44,** 41–60.

Kanzaki, H., Saitoh, H., Ito, A., Fujisawa, S., Kamoun, S., Katou, S., Yoshioka, H., and Terauchi, R. (2003). Cytosolic HSP90 and HSP70 are essential components of INF1-mediated hypersensitive response and non-host resistance to *Pseudomonas cichorii* in *Nicotiana benthamiana.* Mol. Plant Pathol. **4,** 383–391.

Keates, S.E., Kostman, T.A., Anderson, J.D., and Bailey, B.A. (2003). Altered gene expression in three plant species in response to treatment with Nep1, a fungal protein that causes necrosis. Plant Physiol. **132,** 1610–1622.

Kim, M.G., da Cunha, L., McFall, A.J., Belkhadir, Y., DebRoy, S., Dangl, J.L., and Mackey, D. (2005). Two *Pseudomonas syringae* type III effectors inhibit RIN4-regulated basal defense in *Arabidopsis.* Cell **121,** 749–759.

Kumar, S., Tamura, K., and Nei, M. (2004). MEGA3: Integrated software for molecular rvolutionary genetics analysis and sequence alignment. Brief. Bioinform. **5,** 150–163.

Lam, E. (2004). Controlled cell death, plant survival and development. Nat. Rev. Mol. Cell Biol. **5,** 305–315.

Lam, E., and del Pozo, O. (2000). Caspase-like protease involvement in the control of plant cell death. Plant Mol. Biol. **44,** 417–428.

Lee, J., Klüsener, B., Tsiamis, G., Stevens, C., Neyt, C., Tampakaki, A.P., Panopoulos, N.J., Noller, J., Weiler, E.W., Cornelis, G.R., Mansfield, J.W., and Nürnberger, T. (2001). HrpZ(Psph) from the plant pathogen *Pseudomonas syringae* pv. *phaseolicola* binds to lipid bilayers and forms an ion-conducting pore in vitro. Proc. Natl. Acad. Sci. USA **98,** 289–294.

Manning, V.A., and Ciuffetti, L.M. (2005). Localization of Ptr ToxA produced by *Pyrenophora tritici-repentis* reveals protein import into wheat mesophyll cells. Plant Cell **17,** 3203–3212.

Marchler-Bauer, A., et al. (2005). CDD: A Conserved Domain Database for protein classification. Nucleic Acids Res. **33,** 192–196.

Mattinen, L., Tshuikina, M., Mae, A., and Pirhonen, M. (2004). Identification and characterization of Nip, necrosis-inducing virulence protein of *Erwinia carotovora* subsp. *carotovora.* Mol. Plant Microbe Interact. **17,** 1366–1375.

Nühse, T.S., Peck, S.C., Hirt, H., and Boller, T. (2000). Microbial elicitors induce activation and dual phosphorylation of the *Arabidopsis thaliana* MAPK 6. J. Biol. Chem. **275,** 7521–7526.

Nürnberger, T., Brunner, F., Kemmerling, B., and Piater, L. (2004). Innate immunity in plants and animals: Striking similarities and obvious differences. Immunol. Rev. **198,** 249–266.

Nürnberger, T., Nennstiel, D., Jabs, T., Sacks, W.R., Hahlbrock, K., and Scheel, D. (1994). High affinity binding of a fungal oligopeptide elicitor to parsley plasma membranes triggers multiple defense responses. Cell **78,** 449–460.

Oka, K., Akamatsu, H., Kodama, M., Nakajima, H., Kawada, T., and Otani, H. (2005). Host-specific AB-toxin production by germinating spores of *Alternaria brassicicola* is induced by a host-derived oligosaccharide. Physiol. Mol. Plant Biol. **66,** 12–19.

Parker, M.W., and Feil, S.C. (2005). Pore-forming protein toxins: From structure to function. Prog. Biophys. Mol. Biol. **88,** 91–142.

Peart, J.R., et al. (2002). Ubiquitin ligase-associated protein SGT1 is required for host and nonhost disease resistance in plants. Proc. Natl. Acad. Sci. USA **99,** 10865–10869.

Pedley, K.F., and Martin, G.B. (2005). Role of mitogen-activated protein kinases in plant immunity. Curr. Opin. Plant Biol. **8,** 541–547.

Pemberton, C.L., and Salmond, G.P.C. (2004). The Nep1-like proteins - A growing family of microbial elicitors of plant necrosis. Mol. Plant Pathol. **5,** 353–359.

Pemberton, C.L., Whitehead, N.A., Sebaihia, M., Bell, K.S., Hyman, L.J., Harris, S.J., Matlin, A.J., Robson, N.D., Birch, P.R., Carr, J.P., Toth, I.K., and Salmond, G.P. (2005). Novel quorum-sensing-controlled genes in *Erwinia carotovora* subsp. *carotovora*: Identification of a fungal elicitor homologue in a soft-rotting bacterium. Mol. Plant Microbe Interact. **18,** 343–353.

Pieterse, C.M., and Van Loon, L.C. (2004). NPR1: The spider in the web of induced resistance signaling pathways. Curr. Opin. Plant Biol. **7,** 456–464.

Quayyum, H., Gijzen, M., and Traquair, J. (2003). Purification of a necrosis-inducing, host-specific protein toxin from spore germination fluid of *Alternaria panax.* Phytopathol. **93,** 323–328.

Qutob, D., Kamoun, S., and Gijzen, M. (2002). Expression of a *Phytophthora sojae* necrosis inducing protein occurs during transition from biotrophy to necrotrophy. Plant J. **32,** 361–373.

Racape, J., Belbahri, L., Engelhardt, S., Lacombe, B., Lee, J., Lochman, J., Marais, A., Nicole, M., Nürnberger, T., Parlange, F., Puverel, S., and Keller, H. (2005). Ca^{2+}-dependent lipid binding and membrane integration of PopA, a harpin-like elicitor of the hypersensitive response in tobacco. Mol. Microbiol. **58,** 1406–1420.

Ratner, A.J., Hippe, K.R., Aguilar, J.L., Bender, M.H., Nelson, A.L., and Weiser, J.N. (2006). Epithelial cells are sensitive detectors of bacterial pore-forming toxins. J. Biol. Chem. **281,** 12994–12998.

Ron, M., and Avni, A. (2004). The receptor for the fungal elicitor ethylene-inducing xylanase is a member of a resistance-like gene family in tomato. Plant Cell **16,** 1604–1615.

Sasabe, M., Takeuchi, K., Kamoun, S., Ichinose, Y., Govers, F., Toyoda, K., Shiraishi, T., and Yamada, T. (2000). Independent pathways leading to apoptotic cell death, oxidative burst and defense gene expression in response to elicitin in tobacco cell suspension culture. Eur. J. Biochem. **267,** 5005–5013.

Schaller, A., and Oecking, C. (1999). Modulation of plasma membrane H^+-ATPase activity differentially activates wound and pathogen defense responses in tomato plants. Plant Cell **11,** 263–272.

Schmid, M., Davison, T.S., Henz, S.R., Pape, U.J., Demar, M., Vingron, M., Schölkopf, B., Weigel, D., and Lohmann, J.U. (2005). A gene expression map of *Arabidopsis thaliana* development. Nat. Genet. **37,** 501–506.

Schmidt, K., Heberle, B., Kurrasch, J., Nehls, R., and Stahl, D.J. (2004). Suppression of phenylalanine ammonia lyase expression in sugar beet by the fungal pathogen *Cercospora beticola* is mediated at the core promoter of the gene. Plant Mol. Biol. **55,** 835–852.

Shiu, S.H., Karlowski, W.M., Pan, R., Tzeng, Y.H., Mayer, K.F., and Li, W.H. (2004). Comparative analysis of the receptor-like kinase family in *Arabidopsis* and rice. Plant Cell **16,** 1220–1234.

Srivastava, A., Henneke, P., Visintin, A., Morse, S.C., Martin, V., Watkins, C., Paton, J.C., Wessels, M.R., Golenbock, D.T., and Malley, R. (2005). The apoptotic response to pneumolysin is Toll-like receptor 4 dependent and protects against pneumococcal disease. Infect. Immun. **73,** 6479–6487.

Stone, J.M., Heard, J.E., Asai, T., and Ausubel, F.M. (2000). Simulation of fungal-mediated cell death by fumonisin B1 and selection of fumonisin B1-resistant (fbr) *Arabidopsis* mutants. Plant Cell **12,** 1811–1822.

Tada, Y., Kusaka, K., Betsuyaku, S., Shinogi, T., Sakamoto, M., Ohura, Y., Hata, S., Mori, T., Tosa, Y., and Mayama, S. (2005). Victorin triggers programmed cell death and the defense response via interaction with a cell surface mediator. Plant Cell Physiol. **46,** 1787–1798.

Takahashi, A., Casais, C., Ichimura, K., and Shirasu, K. (2003). HSP90 interacts with RAR1 and SGT1 and is essential for RPS2-mediated disease resistance in *Arabidopsis.* Proc. Natl. Acad. Sci. USA **100,** 11777–11782.

Tolleson, W.H., Couch, L.H., Melchior, W.B., Jr., Jenkins, G.R., Muskhelishvili, M., Muskhelishvili, L., McGarrity, L.J., Domon, O., Morris, S.M., and Howard, P.C. (1999). Fumonisin B1 induces apoptosis in cultured human keratinocytes through sphinganine accumulation and ceramide depletion. Int. J. Oncol. **14,** 833–843.

Torres, M.A., and Dangl, J.L. (2005). Functions of the respiratory burst oxidase in biotic interactions, abiotic stress and development. Curr. Opin. Plant Biol. **8,** 397–403.

van't Slot, K., and Knogge, W. (2002). A dual role for microbial pathogen-derived effector proteins in plant disease and resistance. Crit. Rev. Plant Sci. **21,** 229–271.

Veit, S., Wörle, J.M., Nürnberger, T., Koch, W., and Seitz, H.U. (2001). A novel protein elicitor (PaNie) from *Pythium aphanidermatum* induces multiple defense responses in carrot, *Arabidopsis*, and tobacco. Plant Physiol. **127,** 832–841.

Vorwerk, S., Somerville, S., and Somerville, C. (2004). The role of plant cell wall polysaccharide composition in disease resistance. Trends Plant Sci. **9,** 203–209.

Wang, J.Y., Cai, Y., Gou, J.Y., Mao, Y.B., Xu, Y.H., Jiang, W.H., and Chen, X.Y. (2004). VdNEP, an elicitor from *Verticillium dahliae*, induces cotton plant wilting. Appl. Environ. Microbiol. **70,** 4989–4995.

Wang, W., Jones, C., Ciacci-Zanella, J., Holt, T., Gilchrist, D.G., and Dickman, M.B. (1996). Fumonisins and *Alternaria alternata lycopersici* toxins: Sphinganine analog mycotoxins induce apoptosis in monkey kidney cells. Proc. Natl. Acad. Sci. USA **93,** 3461–3465.

Watanabe, N., and Lam, E. (2006). *Arabidopsis* Bax inhibitor-1 functions as an attenuator of biotic and abiotic types of cell death. Plant J. **45,** 884–894.

Wolpert, T.J., Dunkle, L.D., and Ciuffetti, L.M. (2002). Host-selective toxins and avirulence determinants: What's in a name? Annu. Rev. Phytopathol. **40,** 251–285.

Wurtele, M., Jelich-Ottmann, C., Wittinghofer, A., and Oecking, C. (2003). Structural view of a fungal toxin acting on a 14-3-3 regulatory complex. EMBO J. **22,** 987–994.

Xu, Q., and Reed, J.C. (1998). Bax inhibitor-1, a mammalian apoptosis suppressor identified by functional screening in yeast. Mol. Cell **1,** 337–346.

Zeidler, D., Zähringer, U., Gerber, I., Dubery, I., Hartung, T., Bors, W., Hutzler, P., and Durner, J. (2004). Innate immunity in *Arabidopsis thaliana*: Lipopolysaccharides activate nitric oxide synthase (NOS) and induce defense genes. Proc. Natl. Acad. Sci. USA **101,** 15811–15816.

Zipfel, C., and Felix, G. (2005). Plants and animals: A different taste for microbes? Curr. Opin. Plant Biol. **8,** 353–360.

Zipfel, C., Kunze, K., Chinchilla, D., Caniard, A., Jones, J.D.G., Boller, T., and Felix, G. (2006). Perception of the bacterial PAMP EF-Tu by the *Arabidopsis* receptor kinase EFR restricts *Agrobacterium*-mediated transformation. Cell **125,** 749–760.

Zipfel, C., Robatzek, S., Navarro, L., Oakeley, E.J., Jones, J.D., Felix, G., and Boller, T. (2004). Bacterial disease resistance in *Arabidopsis* through flagellin perception. Nature **428,** 764–767.